1972

Finite Element Analysis by Structure Iteration

Richard William Macek

FINITE ELEMENT ANALYSIS
BY STRUCTURE ITERATION

BY

RICHARD WILLIAM MACEK

A thesis submitted
in partial fulfillment of the requirements for
the degree Master of Science, Major in
Mechanical Engineering, South Dakota
State University

1972

FINITE ELEMENT ANALYSIS BY STRUCTURE ITERATION

This thesis is approved as a creditable and independent investigation by a candidate for the degree, Master of Science, and is acceptable as meeting the thesis requirements for this degree, but without implying that the conclusions reached by the candidate are necessarily the conclusions of the major department.

Thesis Advisor Date

Head, Mechanical Engineering Department Date

ACKNOWLEDGMENT

The author wishes to express his appreciation to Dr. Davor Juricic for initiating this problem and for his patient guidance and counseling.

The author also wishes to thank Professor John Sandfort for his guidance throughout the author's graduate program.

RWM

ABSTRACT

A new approach in the application of the Finite Element Method to determine the stress distribution in stress concentration zones has been proposed and investigated. This approach uses the forces on the elements relatively far removed from the concentration zone to obtain the stresses near the zone by an iterative procedure, "Iterative Shrinking." For certain geometries applicable to high concentration zones, i.e. singularities in the stress field, it was shown that the basic equation of "Iterative Shrinking" reduces to simply the remultiplying of the starting matrices. In this case, termed "Conformal Shrinking," the computational effort reduces considerably.

The problem of a finite line crack in an infinite plate, which has a theoretical solution, was solved by "Conformal Shrinking" to test the accuracy of this approach. The variation of the "Conformal Shrinking" solutions with the structural geometry of the finite element divisions was investigated. It was found that the "Iterative Shrinking" solutions vary with the geometry parameters; however, the variation was around the theoretical solution. The structural geometries leading to the optimal solution was pointed out. Although the basic geometry was relatively crude as dictated by the computer time available, the solution contains a 10% error in the criteria parameters chosen.

NOMENCLATURE

$[b]$	Expanded strain relation matrix for structure
$[b]^e$	Element strain relation matrix
$[b^*]$	Element strain relation matrix normalized
c	Half the crack length
$\{e\}$	Expanded strain matrix for structure
$\{e\}^e$	Element strain matrix
$[k]$	Expanded stiffness matrix for structure
$[k]^e$	Element stiffness matrix
$\{s\}$	Expanded nodal force matrix for structure
$\{s\}^e$	Element nodal force matrix
$\{u\}$	Expanded nodal displacement matrix for structure
$\{u\}^e$	Element nodal force matrix
z	Complex coordinate
$\bar{z}$	Complex conjugate of z
$[A]$	Transformation matrix defined by Eq. (2-17)
$[AT]$	Transformation matrix defined by Eq. (3-4)
$[B]_n$	Force relation matrix for nth iterative structure defined by Eq. (3-15)
$\{F\}_n$	Loading matrix for nth iterative structure
$[K]$	Structural stiffness matrix
$[N]$	Element shape function matrix
$\{P\}$	Structural loading matrix
$[R]_n$	Force relation matrix for nth iterative structure defined by Eq. (3-11)
$\{S\}$	Stress at infinity
$\{U\}$	Structural nodal displacement matrix

α	"Shrinking Ratio" for structures
β	"Inner Ring Ratio"; angular displacement
ϵ	Strains
η	Normalized coordinate
$[\kappa]$	Expanded matrix of material constants for structure
$[\kappa]^e$	Matrix of material constants for an element
ν	Poisson's ratio
ξ	Normalized coordinate
ζ	Complex coordinate in elliptical coordinates
$\{\sigma\}$	Expanded stress matrix for structure
$\{\sigma\}^e$	Element stress matrix
σ_x	Normal stress in x direction
σ_y	Normal stress in y direction
τ_{xy}	Shear stress
$\chi(z), \psi(z)$	Complex potentials

LIST OF FIGURES

CONTENTS

CHAPTER I

INTRODUCTION

Stress analysis is perhaps the most crucial aspect in the design of most machine elements. The very foundation of all stress analysis is the theoey of elasticity whose basic governing equations were formulated over one hundred years ago. These equations consist of 3 equilibrium equations, 6 strain-compatibility equations, and 6 stress-strain relations (generalized Hooke's Law). These fifteen basic equations can be combined to form a smaller set of partial differential equations leading to the Beltrami-Mitchell compatability equations or the Navier equations. Even with the simplification of the governing equations, most elasticity problems are too complex for a closed form analytical solution. The problems that have been solved and presented in the many references on the theory of elasticity [1,2] are the problems which are geometrically very simple. Problems with irregular boundary conditions, and, especially problems involving a finite continuum with cutouts, have eluded exact mathematical solutions for all but the simplest forms. To obtain approximate solutions for engineering applications, numerical methods are used.

The approximate numerical methods used are based on either energy consideration (Rayleigh-Ritz), equilibrium

consideration (Finite Elements), or the numerical solution of the governing differential equations (Finite Difference, and weighted-residual methods). Of all these methods, the Finite Element approach treats the problem with irregular boundary conditions the easiest. It is perhaps the most attractive for the engineering analyst since it uses a pure engineering approach and requires a very simple preparation of initial data. The method does, however, require considerable data storage and processing and is, therefore, only feasible when a large, high speed digital computer is available. At present, this method is also finding applications outside the fields of elasticity and structural mechanics.

The finite element method as used in elasticity is based on the assumption that any elastic continuum can be closely approximated by an assemblage of finite elastic elements interconnected at various points called nodes. It is through these nodal points that the forces from one element are transfered to the surrounding elements. The only requirement at the nodes is that there should be equilibrium of forces and continuity of displacement; at positions along the interfaces between elements these conditions need not be satisfied as the size of the element is assumed to be small. The only requirement within an element is compatability of strain. This condition can be easily satisfied

by assuming a simple displacement field such as linearly varying.

In regions of rapidly changing stresses such as around the cutouts shown in figure (1-1), the accuracy of the finite element method using a coarse element division is impared due to the simple element displacement field assumed. One method of circumventing this problem is to employ a finer element subdivision in these areas [5], but this approach necessitates more nodes and elements and hence more computer storage and processing. Unless a large computer is available, this method is usually limited to problems with relatively low stress concentration factors.

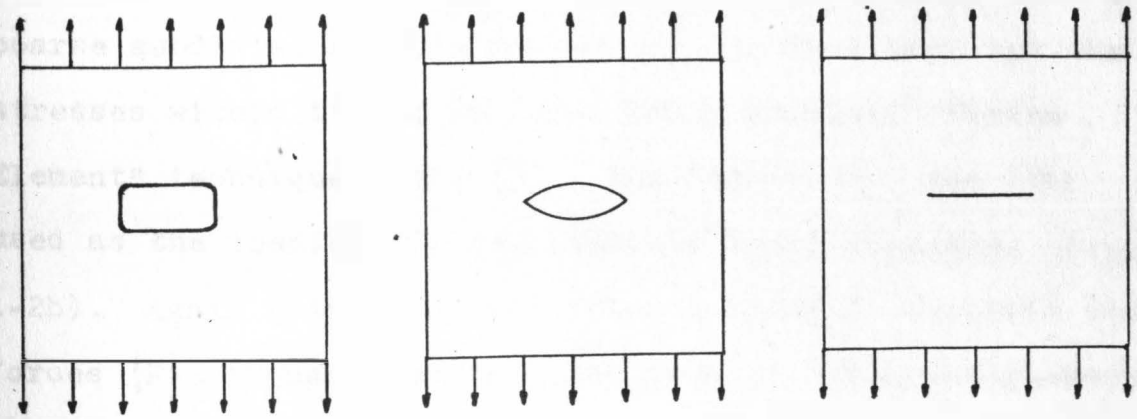

Fig. (1-1) Stress concentration zones.

To overcome this necessity for a large number of elements in areas of rapidly changing stresses, a new approach to the problem of stress concentration using finite elements is being proposed here. This new approach, termed "Iterative

Shrinking", is based on the principle of Saint-Venant, which states that areas with high self-equilibrating stresses only slightly affect the stresses at points far removed from these areas. In terms of finite element methods this means that stresses at point far from stress concentration areas can be accurately determined by using a coarse element division for the structure. The "Iterative Shrinking" approach proposes to use these stresses at points far from these stress concentration areas to determine, in a step by step manner, the stresses near these areas.

As shown in figure (1-2a), the continuum is divided into elements with a thin band of elements at a distance far enough away from the highly stressed area so that the stresses in this band can be determined accurately with a coarse subdivision. The forces $\{F\}_1$ on this band and the stresses within it can be found using standard "Finite Element" technique, Ref. [3]. The forces $\{F\}_1$ are then used as the loading for the band and inner structure (figure 1-2b). Again using standard "Finite Element" analysis the forces $\{F\}_2$ transmitted from the band to the inner elements (figure 1-2c) are found. The assemblage of inner elements is then replaced by a structure similar to the original band and inner element subdivision (figure 1-2d). By the principle of Saint-Venant, these loading forces $\{F\}_2$ transmitted from the original band should be a very good approximation to the

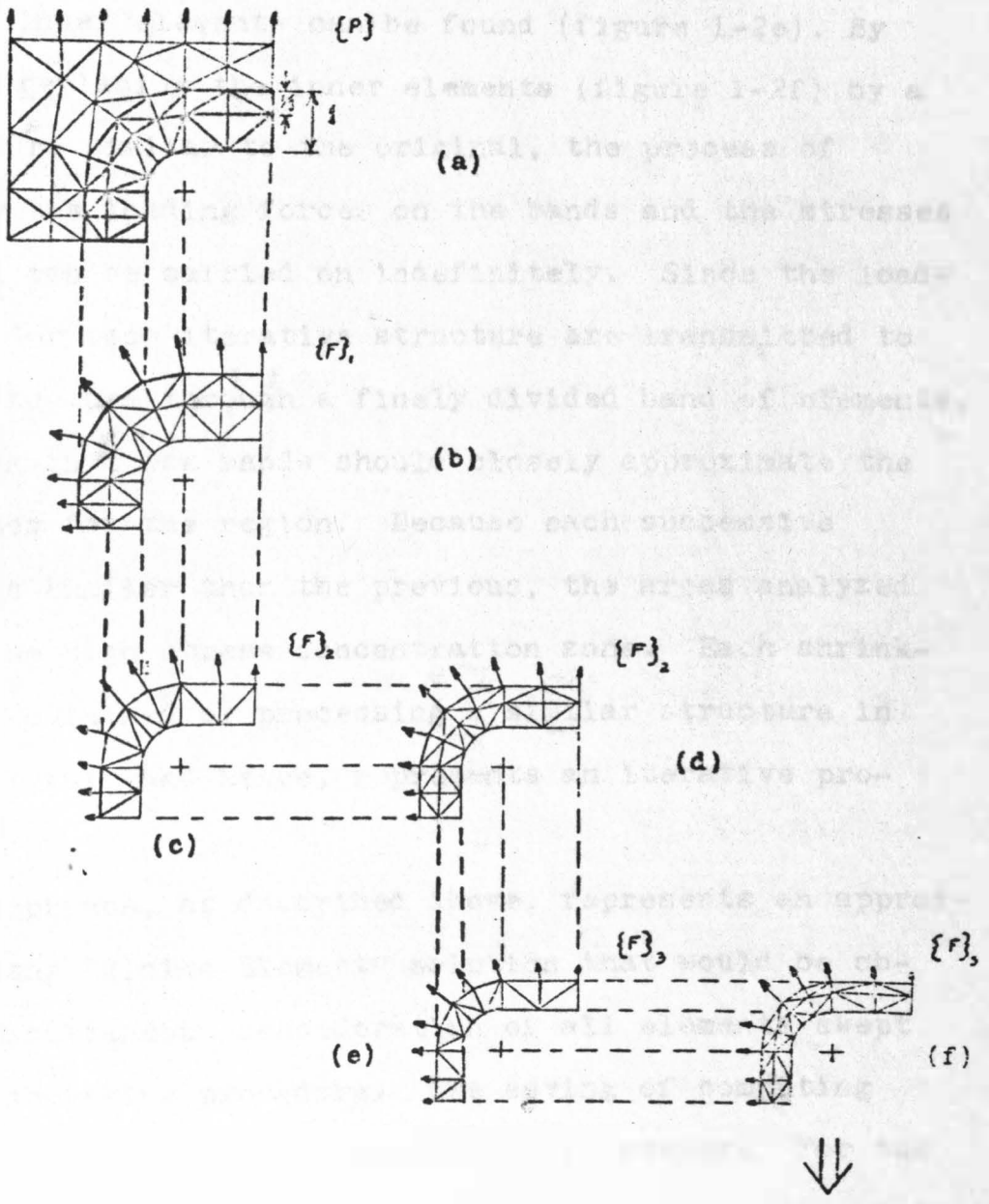

Fig. (1-2) "Iterative Shrinking"

actual loading on this new structure. Again the loading forces $\{F\}_3$ transmitted from the band of this new structure to its inner elements can be found (figure 1-2e). By continually replacing the inner elements (figure 1-2f) by a band structure similar to the original, the process of determining the loading forces on the bands and the stresses within them can be carried on indefinitely. Since the loading forces for each iterative structure are transmitted to the next structure through a finely divided band of elements, the stresses in these bands should closely approximate the true stresses for the region. Because each successive structure is smaller than the previous, the areas analyzed shrink to the high stress concentration zone. Each shrinking step is obtained by processing a similar structure in an identical way, and hence, represents an iterative procedure.

This approach, as described above, represents an approximation to the "Finite Element" solution that would be obtained by simultaneous consideration of all elements swept during the shrinking procedure. The saving of computing time and required memory is considerable, however. For the illustrated example (figure 1-2), a ten iteration process that would determine the stresses at distances up to two-hundredths of the structure width away from the boundary of the highly stressed area would require only one-30th the memory and

one-20th the amount of processing time. This makes the "Iterative Shrinking" approach, even as an approximation to the full "Finite Element" solution, worthwhile considering.

The purpose of the thesis presented on the following pages is to develop and partially evaluate this approach. The presentation consists primarily of the following topics: (a) presentation of the basic equations for the displacement formulation of the "Finite Element" method, (b) development of the basic equations for two-dimensional "Iterative Shrinking" procedure, (c) simplification of "Iterative Shrinking" for cases when "Conformal Shrinking" can be applied, (d) solution of a simple problem which has a known theoretical solution, (e) the investigation of the influence of several computational parameters on the accuracy of the solution. All considerations are restricted to plane problems for an ideally elastic continuum.

The conclusions and recommendations presented in this thesis were based on the evaluation of only one simple problem using this technique. Since the accuracy of finite element methods is primarily empirically tested, a wide variety of problems should be attempted before any general conclusion, as to the merit of this technique, is reached.

CHAPTER II

THE DISPLACEMENT FORMULATION OF THE FINITE ELEMENT METHOD

As stated in the introduction, the basis of all finite element methods in the solution of elasticity problems is the assumption that an elastic continuum can be closely approximated by an assemblage of a finite number of elastic elements interconnected at a discrete number of nodal points. If the nodal force-displacement relationships for the individual elements are known, it is possible by using various well-known methods of structural analysis (see Ref. [4]), to obtain an approximate stress distribution for the continuum.

As stated by Zienkiewicz in reference [3], the approximation of the continuum using finite elements is made in the following manner:

(a) The continuum is separated by imaginary lines or surfaces into a number of "finite elements".

(b) The elements are assumed to be interconnected at a discrete number of nodal points situated on their boundaries. The displacements of these nodal points will be the basic unknown parameters, just as in structural analysis.

(c) A function is chosen to define uniquely the state of displacement within each "finite element" in terms of its nodal displacements.

(d) The displacement function now uniquely defines the

state of strain within an element in terms of the nodal displacements. The strains and the elastic properties of the material will define the state of stress throughout the element.

(e) A system of forces concentrated at the nodes and equivalent to the stresses assumed is determined, resulting in a nodal force-displacement or a stiffness relationship.

Once this has been completed the solution procedure follows the routine of matrix structural analysis.

The main equations and procedure of the matrix displacement method, as used later in the analysis of the "Iterative Shrinking" concept, are exposed in the following paragraphs of this chapter. The presentation follows the outline and notation of reference [4]. A simple plane triangular element is considered first, followed by the relations for a continuum-structure composed of finite elements.

A typical element e of a structure, such as the one in figure (2-1), is defined by nodes one, two, three and the straight line boundaries. The displacements at any point within the element are defined by a column vector, $\{u(x,y)\}$. In terms of the nodal displacements $\{u\}^e$,

$$\{u(x,y)\} = [N] \{u\}^e \qquad \text{Eq. (2-1)}$$

where the terms of $[N]$ are in general functions of the position coordinates, x and y.

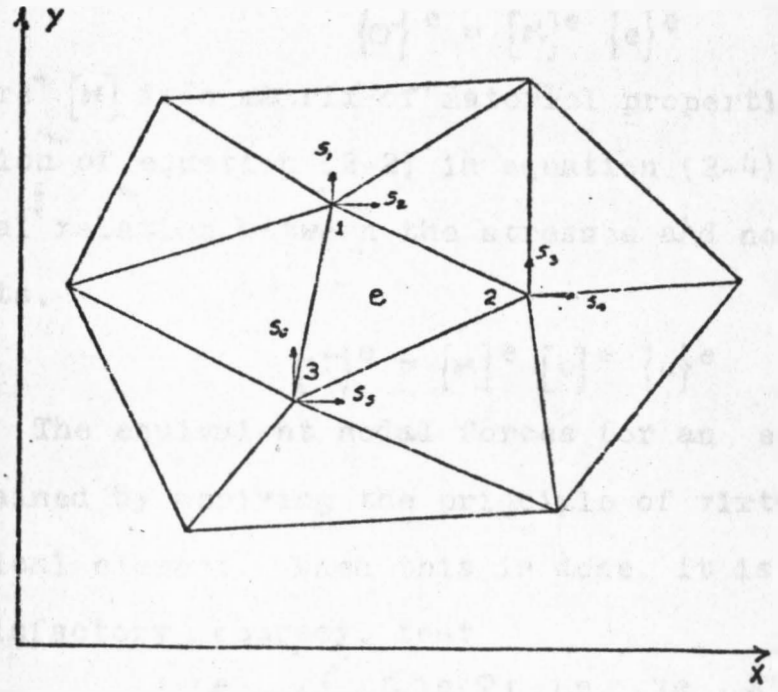

Fig. (2-1) Representative structure and elements.

By differentiating equation (2-1), the strains $\{e\}^e$ within the element are found. This results in a relationship which can be written in matrix form as

$$\{e\}^e = [b]^e \{u\}^e \qquad \text{Eq. (2-2)}$$

where, for plane problems,

$$\{e\}^e = \begin{Bmatrix} \epsilon_x \\ \epsilon_y \\ \epsilon_{xy} \end{Bmatrix} = \begin{Bmatrix} \frac{\partial u_x}{\partial x} \\ \frac{\partial u_y}{\partial y} \\ \frac{\partial u_x}{\partial y} + \frac{\partial u_y}{\partial x} \end{Bmatrix} \qquad \text{Eq. (2-3)}$$

and again the terms of $[b]^e$ are in general functions of the position coordinates.

If initial strains and thermal strains are neglected and linear elastic behaviour assumed, the relationship between stress and strain is linear and of the form

$$\{\sigma\}^e = [\varkappa]^e \{e\}^e \qquad \text{Eq. (2-4)}$$

where $[\varkappa]$ is a matrix of material properties. By substitution of equation (2-2) in equation (2-4), we get the final relation between the stresses and nodal displacements,

$$\{\sigma\}^e = [\varkappa]^e [b]^e \{u\}^e \qquad \text{Eq. (2-5)}$$

The equivalent nodal forces for an element $\{s\}^e$ are obtained by applying the principle of virtual work to a typical element. When this is done, it is found, with a satisfactory accuracy, that

$$\{s\}^e = (\int_V ([b]^e)^T [\varkappa]^e [b]^e \, dV) \{u\}^e \qquad \text{Eq. (2-6)}$$

This relationship is usually expressed in the following manner:

$$\{s\}^e = [k]^e \{u\}^e \qquad \text{Eq. (2-7)}$$

where the element stiffness matrix $[k]^e$ is found by using

$$[k]^e = \int_V ([b]^e)^T [\varkappa]^e [b]^e \, dV \qquad \text{Eq. (2-8)}$$

Equation (2-8) is determined for each element e separately. To consider the complete structure, all these equations (2-5) and (2-7) are combined to form two matrix equations expanded into "structure-size".

$$\{s\} = [k] \{u\} \qquad \text{Eq. (2-9)}$$

$$\{\sigma\} = [\varkappa] [b] \{u\} \qquad \text{Eq. (2-10)}$$

where the "structure-size" matrices are defined as follows:

$$\{s\} = \{ \{s\}^1 \{s\}^2 \ldots \{s\}^e \ldots \} \qquad \text{Eq. (2-11)}$$

$$[k] = [[k]^1 [k]^2 \ldots [k]^e \ldots] \qquad \text{Eq. (2-12)}$$

$$\{u\} = \{\{u\}^1 \{u\}^2 \cdots \{u\}^e \cdots\} \quad \text{Eq. (2-13)}$$

$$[\varkappa] = [[\varkappa]^1 [\varkappa]^2 \cdots [\varkappa]^e \cdots] \quad \text{Eq. (2-14)}$$

$$[b] = [[b]^1 [b]^2 \cdots [b]^e \cdots] \quad \text{Eq. (2-15)}$$

$$\{\sigma\} = \{\{\sigma\}^1 \{\sigma\}^2 \cdots \{\sigma\}^e \cdots\} \quad \text{Eq. (2-16)}$$

The nodal displacements $\{u\}$ for the elements are related to the nodal displacements $\{U\}$ for the composite structure by an equation of the form

$$\{u\} = [A] \{U\} \quad \text{Eq. (2-17)}$$

where $[A]$ is a rectangular matrix in which the terms consist of zeros and ones only. The external loading forces corresponding to the displacements $\{U\}$ are denoted by the matrix $\{P\}$, where

$$\{P\} = [A]^T \{s\} \quad \text{Eq. (2-18)}$$

Substitution of equations (2-9) and (2-17) into equations (2-18) results in

$$\{P\} = [A]^T [k] [A] \{U\}$$

or

$$\{P\} = [K] \{U\} \quad \text{Eq. (2-19)}$$

where

$$[K] = [A]^T [k] [A] \quad \text{Eq. (2-20)}$$

When operating with the matrix $[K]$, the following should be kept in mind. The matrix $[K]$ is the stiffness matrix for the structure regarded as a free body and equation (2-19) represents equations of equilibrium for the element forces acting at all nodes. This implies that the load matrix $\{P\}$ must constitute a set of forces in static

equilibrium. From the consideration of overall equilibrium of the structure, it is clear that there must be three dependent equations, corresponding to the three rigid body degrees of freedom. This dependence renders the $[K]$ matrix singular. To overcome this problem, reference [4] suggests that three displacements at certain selected points on the structure be assumed equal to zero, and the corresponding rows and columns from the complete stiffness matrix $[K]$ be eliminated. The three displacements chosen must be such that all rigid body degrees of freedom are restricted.

The structural stiffness matrix $[K]$ can be calculated without the matrix multiplication

$$[A]^T [k] [A] .$$

This method, called the direct stiffness method, consists of summing the appropriate stiffness terms for the element stiffness matrix $[k]$ and assembling these sums in a proper manner to form the structural stiffness matrix $[K]$.

Equation (2-22) is the basic equation which must be solved for the displacements $\{U\}$ whenever the matrix displacement method is used. From these displacements all stresses and strains in the various elements can be found by using equations (2-17), and (2-10).

CHAPTER III

"ITERATIVE SHRINKING" USING THE DISPLACEMENT METHOD

In chapter two the basic equation of the displacement formulation, the equilibrium equation,

$$\{P\} = [K]\ \{U\} \qquad \text{Eq. (2-19) rep.}$$

or

$$\{U\} = [K]^{-1}\ \{P\} \qquad \text{Eq. (3-1)}$$

was derived. Once the unknown displacements $\{U\}$ are solved, all the stresses and strains in every element can be obtained by the proper matrix operations. It is obvious from the above equations that if even a moderate number of nodes and elements are used, the solution to these equations can represent a formidable computational task.

As stated in the introduction, most displacement fields assumed for elements are very simple. Since strains are obtained from the derivatives of the displacements, the strains and, hence the stresses, will also be of a quite simple form. Regions of rapidly varying stresses will, therefore, necessitate a fine element subdivision in order to closely approximate the true stress distributions. Unless a very large computer is available, problems involving high stress concentrations cannot be accurately solved with this method. Because of this need for prohibitively large computer storage and lengthy process time, a new procedure that leads to an approximate finite element solution, termed "Iterative

Shrinking" has been proposed. The main topic of this thesis, therefore, is to develop and partially evaluate the "Iterative Shrinking" approach.

The conceptual basis of "Iterative Shrinking" is the principle of Saint-Venant, which simply states that regions of high stress concentration, where the stresses are self equilibrated, do not appreciably affect the stress distributions in areas relatively far removed from the stress concentration zone. In terms of finite element methods, this means that the stresses in elements far away from the concentration zone will be only slightly affected by the number of elements used to subdivide the region near the concentration zone. The "Iterative Shrinking" approach proposes to use the stresses and corresponding internal nodal forces from the regions removed from the concentration zone, which can be determined accurately with a coarse element division, to predict the stresses and internal nodal forces nearer the stress concentration zone, by using an iterative computing procedure.

With the above concepts in mind, the "Iterative Shrinking" approach will now be developed and illustrated. A general problem to which this approach might apply is the problem of a cutout in a finite plate such as the one shown in figure (3-1a), with the finite element approximation shown in figure (3-1b). In order for this approach

(a)

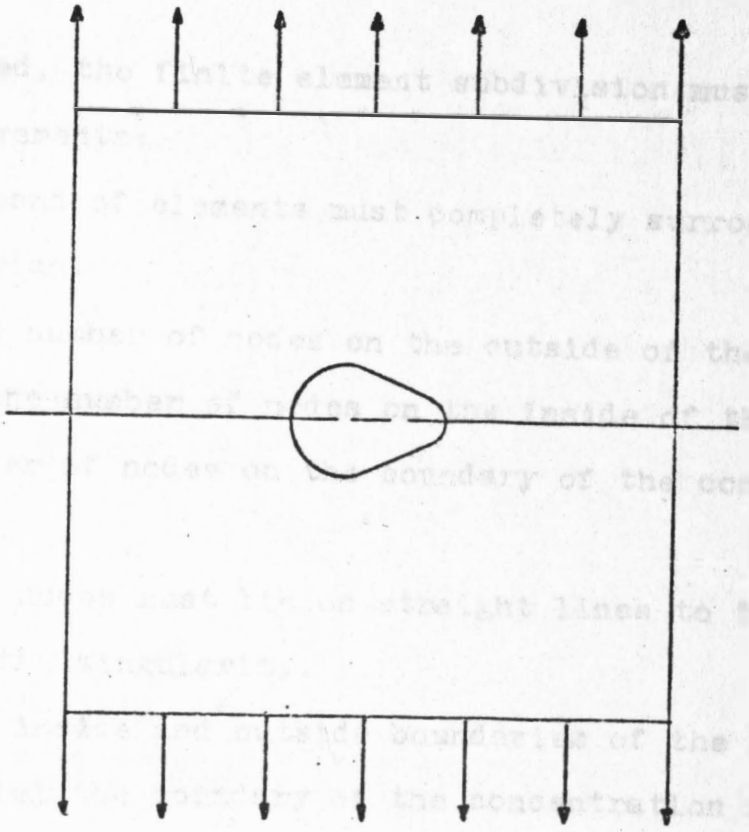

(b)

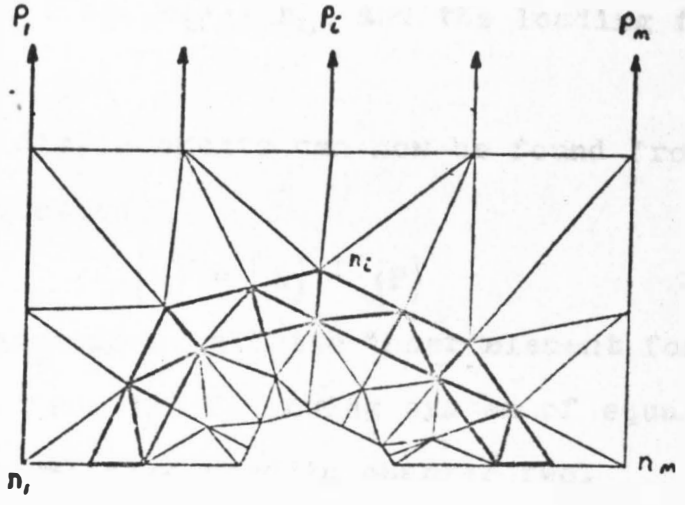

Fig. (3-1) "Iterative Shrinking" example.

to be applied, the finite element subdivision must satisfy these requirements:

(a) A band of elements must completely surround the singular region.

(b) The number of nodes on the outside of the band must equal the number of nodes on the inside of the band and the number of nodes on the boundary of the concentration zone.

(c) The nodes must lie on straight lines to the boundary of the singularity.

(d) The inside and outside boundaries of the band should parallel the boundary of the concentration zone.

All these requirements are met by the problem shown in figure (3-1b). The band of elements is highlighted; the nodes are n_1, n_2, $n_1 \cdots n_m$, and the loading forces are P_1, P_2, $P_1 \cdots P_m$.

The nodal displacements can now be found from the basic matrix equation,

$$\{U\} = [K]^{-1} \{P\} \qquad \text{Eq. (3-1)}$$

Once this has been done, all the inner element forces $\{s\}$ can be obtained from the following system of equations; the matrices used were introduced in chapter two.

$$\{u\} = [A] \{U\} \qquad \text{Eq. (2-17) rep.}$$

$$\{s\} = [k] \{u\} \qquad \text{Eq. (2-9) rep.}$$

If equation (2-17) is substituted into equation (2-9), we get

$$\{s\} = [k][A]\{U\} \qquad \text{Eq. (3-2)}$$

Substituting equation (3-1) into equation (3-2),

$$\{s\} = [k][A][K]^{-1}\{P\} \qquad \text{Eq. (3-3)}$$

The outer structure can now be disregarded and replaced by the forces $\{F\}_1$ which it transmitts to the band and to inner structure as shown in figure (3-2a). The forces $\{F\}_1$ can be obtained from $\{s\}$ by intoducing a new matrix $[AT]$, where

$$\{F\}_1 = [AT]\{s\} \qquad \text{Eq. (3-4)}$$

Substituting equation (3-3) into equation (3-4),

$$\{F\}_1 = [AT][k][A][K]^{-1}\{P\} \qquad \text{Eq. (3-5)}$$

The matrix $[AT]$ is a rectangular matrix, similar to the transformation matrix $[A]$, with terms equal to zeros and ones only. If this substructure is now solved for the displacements using $\{F\}_1$ in place of $\{P\}$ in equation (3-1), i.e.

$$\{U\}_1 = [K]_1^{-1}\{F\}_1 \qquad \text{Eq. (3-6)}$$

The same result will be obtained as when treating the initial full structure. However, in this form it represents the initial structure to which the iterative procedure that follows will be applied, hence the subscript 1. It also corresponds to the structure number in figure (3-2).

Next the loading forces $\{F\}_2$ transmitted from the band to the inner structure can be obtained from an

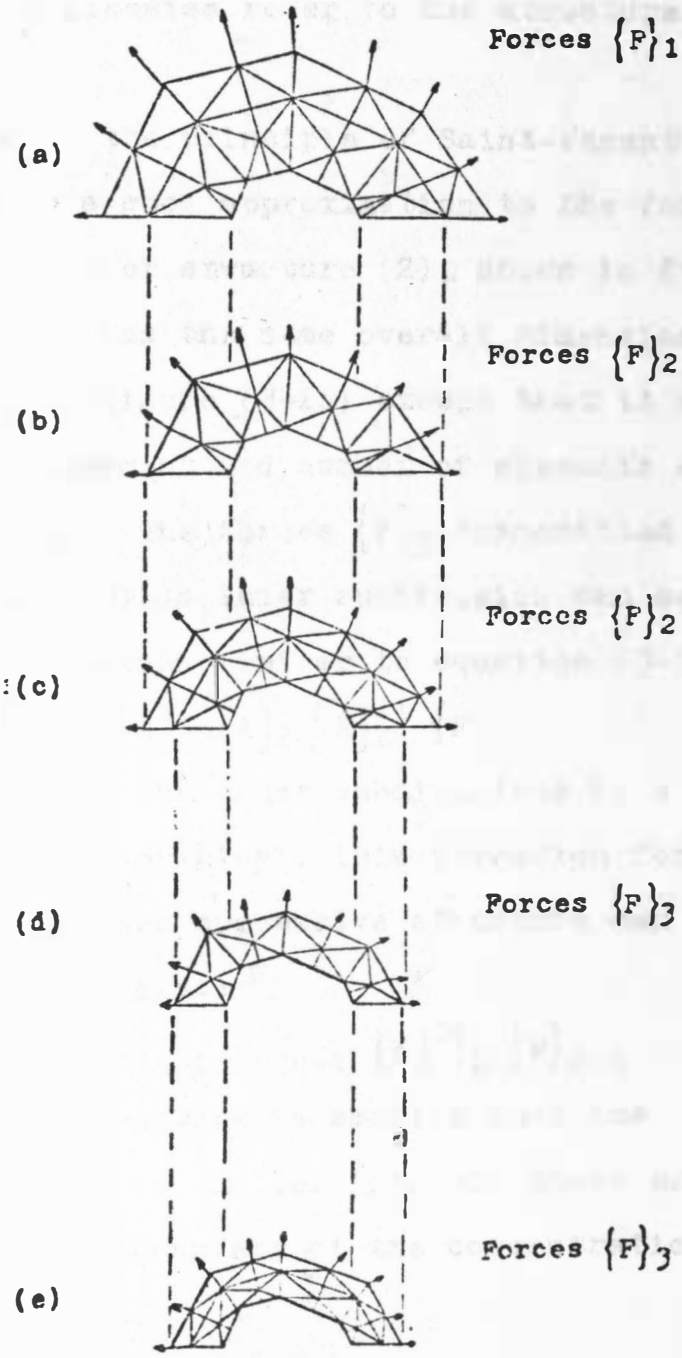

Fig. (3-2) Shrinking structures.

equation analogous to equation (3-5):

$$\{F\}_2 = [AT]_1 \; [k]_1 \; [A]_1 \; [K]_1^{-1} \; \{F\}_1 \quad \text{Eq. (3-7)}$$

where the subscripts likewise refer to the structure number.

Now, according to the principle of Saint-Venant, the forces $\{F\}_2$ should be a good approximation to the forces actually acting on a finer structure (2), shown in figure (3-2c). Structure (2) has the same overall dimensions as the structure shown in figure (3-2b) except that it has the same element arrangement and number of elements as the original structure (1). The forces $\{F\}_3$ transmitted from the band of structure (2) to inner subdivision can again be obtained from an equation similar to equation (3-7):

$$\{F\}_3 = [AT]_2 \; [k]_2 \; [A]_2 \; [K]_2^{-1} \; \{F\}_2$$

By continually replacing the inner subdivisions by a band structure similar to the original, this iteration for the loading forces $\{F\}_n$ on each successive structure can be carried on indefinitely, i.e.:

$$\{F\}_n = [AT]_{n-1} \; [k]_{n-1} \; [A]_{n-1} \; [K]_{n-1}^{-1} \; \{F\}_{n-1}$$

Since each successive structure is smaller than the preceding, the structure is smaller than all those previous and approaches the boundary of the concentration zone. From equation (3-6)

$$\{U\}_n = [K]_n^{-1} \; \{F\}_n \quad \text{Eq. (3-8)}$$

the displacements and, hence the stresses, for each struc-

ture can be found. The stresses in each band can then be used as a good approximation to the actual stresses for the area.

For clarity, this method will now be stated as the following procedure:

(1) The outer structure is removed and replaced by the forces $\{F\}_1$ that it transmitts to the band and inner structure. These forces are given by equation (3-5).

$$\{F\}_1 = [AT][k][A][K]^{-1}\{P\} \quad \text{Eq. (3-5) rep.}$$

(2) The forces $\{F\}_2$ that the band transmitts to the inner structure are likewise obtained by using

$$\{F\}_2 = [AT]_1[k]_1[A]_1[K]_1^{-1}\{F\}_1 \qquad \text{Eq. (3-7)}$$

or

$$\{F\}_2 = [R]_1\{F\}_1 \qquad \text{Eq. (3-9)}$$

where

$$[R]_1 = [AT]_1[k]_1[A]_1[K]_1^{-1}$$

(3) The inner structure is replaced by a finer structure similar to the original.

(4) The forces $\{F\}_3$ that the band of this new structure transmitts are obtained from an equation analogous to (3-9).

$$\{F\}_3 = [R]_2\{F\}_2$$

(5) In general the forces on any shrunken structure (n) can be obtained from an equation similar to (3-5).

$$\{F\}_n = [R]_{n-1}\{F\}_{n-1} \qquad \text{Eq. (3-10)}$$

where

$$[R]_n = [AT]_n [k]_n [A]_n [K]_n^{-1} \qquad \text{Eq. (3-11)}$$

(6) The stresses $\{\sigma\}_n$ can then be found from $\{F\}_n$ in the following manner:

$$\{U\}_n = [K]_n^{-1} \{F\}_n \qquad \text{Eq. (3-8) rep.}$$

by using equation (2-17):

$$\{u\}_n = [A]_n \{U\}_n \qquad \text{Eq. (3-12)}$$

by using equation (2-10):

$$\{\sigma\}_n = [\mathcal{H}]_n [b]_n \{u\}_n \qquad \text{Eq. (3-13)}$$

Substituting equation (3-8) into (3-12) and the results into equation (3-13),

$$\{\sigma\}_n = [\mathcal{H}]_n [b]_n [A]_n [K]_n^{-1} \{F\}_n$$

or

$$\{\sigma\}_n = [B]_n \{F\}_n \qquad \text{Eq. (3-14)}$$

where

$$[B]_n = [\mathcal{H}]_n [b]_n [A]_n [K]_n^{-1} \qquad \text{Eq. (3-15)}$$

The forces $\{F\}_n$ and stresses $\{\sigma\}_n$ can also be related to the forces $\{F\}_1$ on the original structure by using equation (3-10) and the following iteration schemes:

$$\{F\}_n = [R]_{n-1} \{F\}_{n-1}$$
$$\{F\}_n = [R]_{n-1} [R]_{n-2} \{F\}_{n-2}$$
$$\{F\}_n = [R]_{n-1} [R]_{n-2} [R]_{n-3} \{F\}_{n-3}$$

that leads to

$$\{F\}_n = [R]_{n-1} [R]_{n-2} \cdots [R]_1 \{F\}_1 \qquad \text{Eq. (3-16)}$$

Substitution of equation (3-16) into equation (3-14) gives

$$\{\sigma\}_n = [B]_n [R]_{n-1} [R]_{n-2} \cdots [R]_1 \{F\}_1 \qquad \text{Eq. (3-17)}$$

From equation (3-15), it can be seen that the stresses near the concentration zone can be obtained from the forces on the original structure by operating on small structural matrices in an iterative manner. According to the principle of Saint-Venant, these original forces should be quite accurate since the initial band is quite far from the concentration zone. Because the original forces are transmitted to each successive structure through a narrow band of elements with a relatively fine subdivision, the stresses in the bands should closely approximate the true stresses for the region of stress concentration.

In order for the "Iterative Shrinking" method to be readily adaptable to an iterative computation on the digital computer, there should be a convenient way to obtain the nodal coordinates and, hence the stiffness and stress coefficient matrices, for each successive structure. If the requirements for the structure division stated in the first part of the chapter are met, this can be done quite easily as shown below.

Take a typical segment from the original structure (1) with a line of nodes L to the boundary as shown in figure (3-3a).

Typical nodes on the band of structure (1) are i1, j1 and the band of structure (2), i2, j2. The nodes are k1

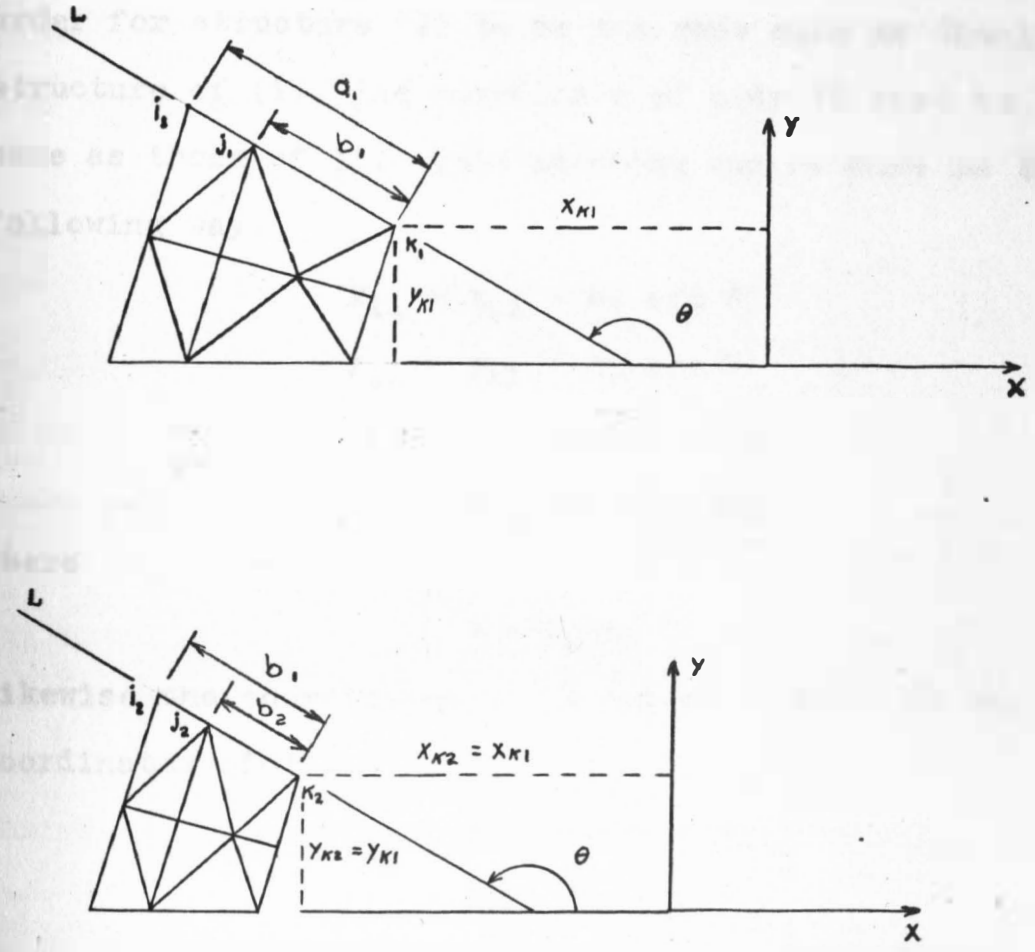

Fig. (3-3) Substructure generation.

and k2 on the boundary of the concentration zone for structures (1) and (2), respectively. For each structure, the coordinates (x_{kn}, y_{kn}) for a node on the boundary must be the same, therefore,

$$x_{k1} = x_{k2} = \cdots = x_{kn}$$

$$y_{k1} = y_{k2} = \cdots = y_{kn}$$

The numerical subscript refers to the structure number and

the alphabetic subscript refers to the node number. In order for structure (2) to be the same size as the inner structure of (1), the coordinate of node i2 must be the same as those of j1. This matching can be done in the following way.

$$x_{i1} = x_{k1} + a_1 \cos\theta$$
$$y_{i1} = y_{k1} + a_1 \sin\theta$$
$$x_{i2} = \alpha a_1 \cos\theta + x_{k1}$$
$$y_{i2} = \alpha a_1 \sin\theta + y_{k1}$$

where

$$\alpha = b_1/a_1$$

Likewise the coordinates of j2 can be related to the coordinates of j1.

$$x_{j2} = \alpha b_1 \cos\theta + x_{k1}$$
$$y_{j2} = \alpha b_1 \cos\theta + y_{k1}$$

In general for the nth iterative structure, with $\alpha = b_n/b_{n-1}$

$$x_{in} = \alpha^{n-1} a_1 \cos\theta + x_{k1}$$
$$y_{in} = \alpha^{n-1} a_1 \sin\theta + y_{k1}$$
$$x_{jn} = \alpha^{n-1} b_1 \cos\theta + x_{k1}$$
$$y_{jn} = \alpha^{n-1} b_1 \sin\theta + y_{k1}$$

Eqs. (3-18)

In the limit as n approaches infinity, both the coordinates for in and jn must approach the coordinates for node kn. Taking the limit of equations (3-18), we see that this is true, as

$$\lim_{n \to \infty} \alpha^{n-1} = 0 \quad \text{for } \alpha < 1$$

Similarly, other "Shrinking Ratios", α, can be determined for each line L of nodes to the boundary of the concentration zone. In this way, the coordinates for all nodes of each successive structure can be obtained from the nodal coordinates of the original structure.

In this chapter, the basic equation of the "Iterative Shrinking" technique, equation (3-17), was derived. Also a convenient way of computing the nodal coordinates and, hence the matrices needed for equation (3-17), was developed. It will be seen in the next chapter that in certain cases the matrices used in the equation can be reduced to matrices depending only upon the original structure. This will greatly simplify the computation necessary in the "Iterative Shrinking" approach, and will generally be applicable in the case of a singular point in the stress field.

CHAPTER IV

CONFORMAL "ITERATIVE SHRINKING"

In chapter three, the basic equation, i.e.

$$\{\sigma\}_n = [B]_n [R]_{n-1} [R]_{n-2} \cdots [R]_1 \{F\}_1 \quad \text{Eq. (3-17) rep.,}$$

of the "Iterative Shrinking" approach was derived. In general for each iteration, new matrices, $[R]_{n-1}$ and $[B]_n$, must be evaluated. It is of interest to investigate conditions under which these matrices could remain the same or differ only by a factor. In this case a great simplification in computation would result, as the iteration procedure would reduce to a remultiplication of only the same matrix.

Consider a case in which all the lines of nodes originate from the same point on the boundary of the concentration zone. In that case, the "Shrinking Ratio" α for the line of node's direction will be also the "Shrinking Ratio" for all other directions within the element, i.e. the element will retain its original form in the process of shrinking to a point on the boundary of the concentration zone. There are many problems which naturally lead to such a "Conformal Shrinking" approach. The problems that lend themselves to this approach are those with sharp edges in the cutout regions (see Fig. 4-1). These sharp edges represent a singular point in the stress field.

The geometric similarity of the successive elements in

the process of "Conformal Shrinking" simplifies the total computation considerably. As shown in the rest of this chapter, the only matrices necessary to perform the iterative shrinking analysis are the starting matrices $[B]_1$,

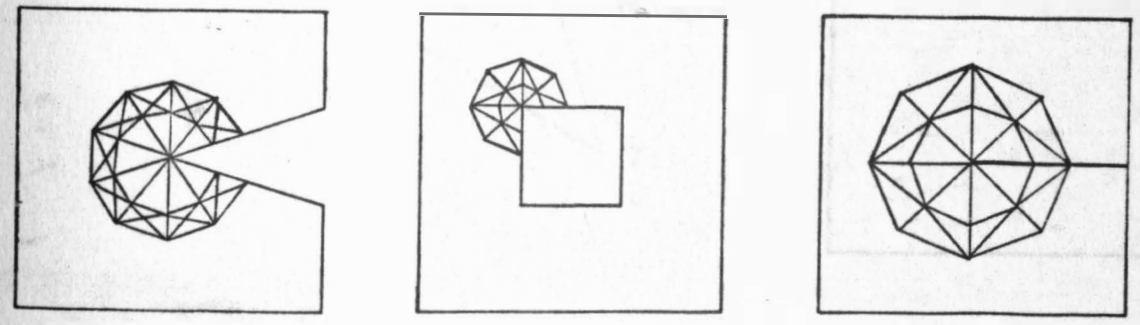

Fig. (4-1) "Conformal Shrinking" geometries.

$[R]_1$, and $\{F\}_1$. The "Conformal Shrinking" process merely consists of remultiplying these matrices.

Since the analogous elements in the "Conformal Shrinking" procedure will be geometrically similar, the stiffness matrices for such two-dimensional elements will be considered first.

Consider two geometrically similar elements as shown in Fig. (4-2). The elements are under plane stress and are of uniform thickness t. According to equation (2-8), the stiffness matrix for the larger element will be

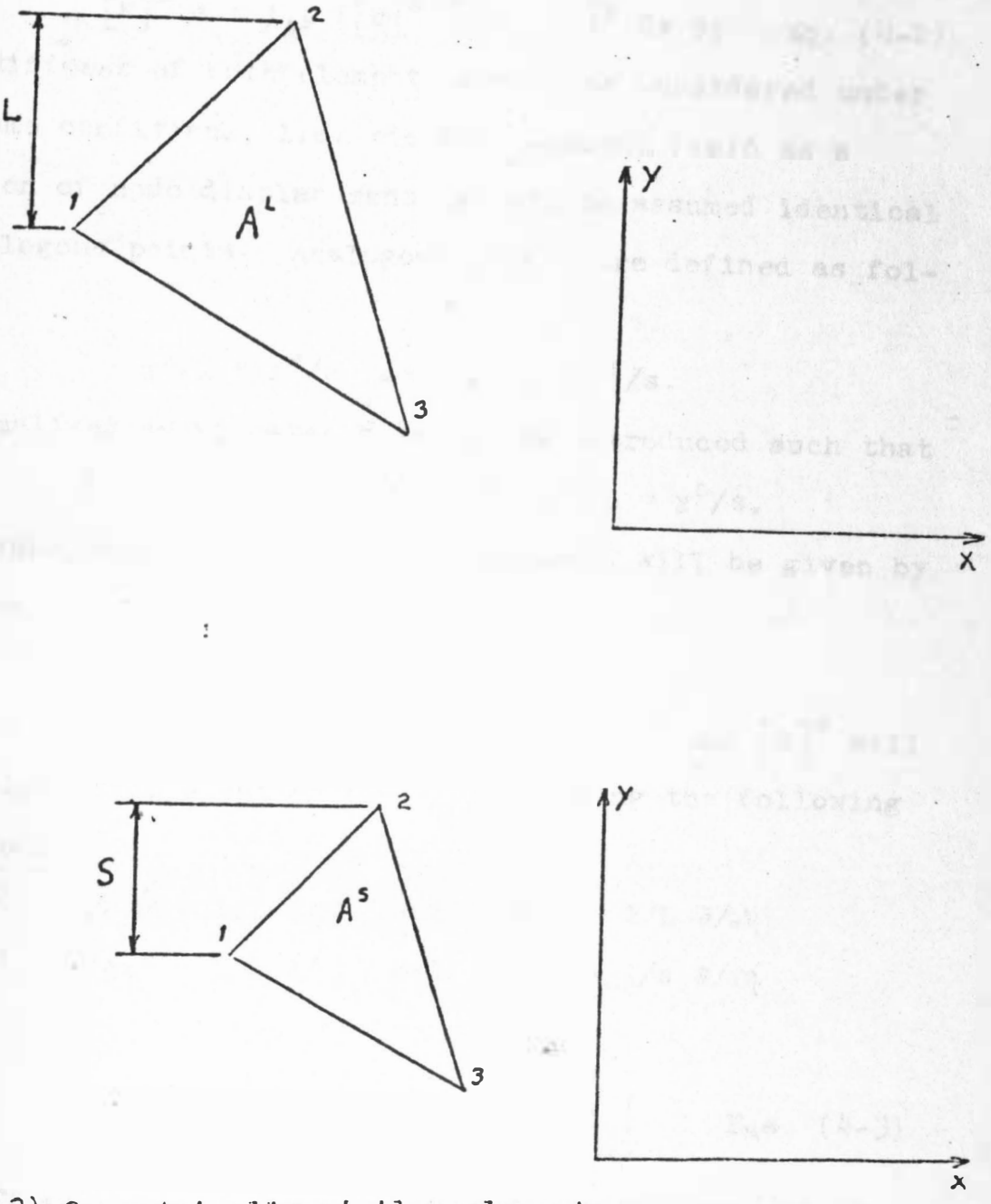

Fig. (4-2) Geometrically similar elements.

$$[k]^L = t \int_{AL} ([b]^L)^T [\varkappa] [b]^L \, dx \, dy \quad \text{Eq. (4-1)}$$

and for the smaller,

$$[k]^s = t \int_{As} ([b]^s)^T [\varkappa] [b]^s \, dx \, dy \quad \text{Eq. (4-2)}$$

The stiffness of both elements should be considered under the same conditions, i.e. the displacement field as a function of node displacements should be assumed identical on analogous points. Analogous points are defined as follows:

$$x^L/L = x^s/s \quad \text{and} \quad y^L/L = y^s/s.$$

If normalized coordinates ξ and η are introduced such that

$$\xi = x^L/L = x^s/s \quad \text{and} \quad \eta = y^L/L = y^s/s,$$

the displacement fields for both elements will be given by equation (2-1) as:

$$\{u(\xi,\eta)\} = [N] \{u\}$$

The strain transformation matrices $[b]^L$ and $[b]^s$ will be obtained from equation (4-1) by applying the following operations:

for $\{e\}^L$ $\quad \partial/\partial x^L = 1/L \; \partial/\partial\xi$ and $\partial/\partial y^L = 1/L \; \partial/\partial\eta$

for $\{e\}^s$ $\quad \partial/\partial x^s = 1/s \; \partial/\partial\xi$ and $\partial/\partial y^s = 1/s \; \partial/\partial\eta$

so that

$$\{e\}^L = [b]^L \{u\} = 1/L \, [b^*] \{u\}$$
$$\{e\}^s = [b]^s \{u\} = 1/s \, [b^*] \{u\} \quad \text{Eqs. (4-3)}$$

where $[b^*]$ is obtained with normalized coordinates and is identical for both elements. These relations for the matrices can now be substituted into equations (4-1) and

(4-2), and the coordinates normalized. This results in

$$[k]^L = t \int_{A_{\xi\eta}} 1/L\ [b']^T [\varkappa]\ 1/L\ [b']\ L^2\ d\xi\ d\eta$$

$$[k]^s = t \int_{A_{\xi\eta}} 1/s\ [b']^T [\varkappa]\ 1/s\ [b']\ s^2\ d\xi\ d\eta$$

Canceling common terms, we see that for geometrically similar elements,

$$[k]^s = [k]^L = t \int_{A_{\xi\eta}} [b']^T [\varkappa] [b']\ d\xi\ d\eta \qquad \text{Eq. (4-4)}$$

i.e. the stiffness matrices will not depend on the element size. Substituting equation (4-4) into equations (2-20) and (2-12) and noting that

$$[AT]_{n-1} = [AT]_{n-2} = \cdots = [AT]_1$$
$$[A]_{n-1} = [A]_{n-2} = \cdots = [A]_1 \qquad \text{Eq. (4-5)}$$

we see that for geometrically similar structures,

$$[k]_{n-1} = [k]_{n-2} = \cdots = [k]_1$$
$$[K]_{n-1} = [K]_{n-2} = \cdots = [K]_1 \qquad \text{Eq. (4-6)}$$

i.e. again the stiffness matrices do not depend on the structure size. Substituting equations (4-5) and (4-6) into equation (3-11) it is seen that for geometrically similar structures

$$[R]_{n-1} = [R]_{n-2} = \cdots = [R]_1. \qquad \text{Eq. (4-7)}$$

We can also see from equation (4-3) that

$$[b]^L = 1/L\ [b']$$
$$[b]^s = 1/s\ [b']$$

or

$$[b]^s = 1/\alpha\ [b]^L$$

and

$$[b]_n = 1/\alpha\,[b]_{n-1}$$
$$[b]_n = 1/\alpha^2\,[b]_{n-2}$$
$$\vdots$$
$$[b]_n = 1/\alpha^{n-1}\,[b]_1 \qquad \text{Eq. (4-8)}$$

where $\alpha = s/L.$

Substitution of equations (4-8), (4-6), and (4-5) into equation (3-15) reveals that

$$[B]_n = 1/\alpha^{n-1}\,[\mathscr{H}]\,[b]_1\,[A]_1\,[K]_1^{-1} \qquad \text{Eq. (4-9)}$$

Substitution of equations (4-9) and (4-7) into equation (3-17), the basic equation for "Iterative Shrinking," gives a simplified iteration equation for "Conformal Shrinking".

$$\{\sigma\}_n = 1/\alpha^{n-1}\,[B]_1\,\underbrace{[R]_1 \cdots [R]_1}_{n-1 \text{ terms}}\,\{F\}_1$$

or

$$\{\sigma\}_n = 1/\alpha^{n-1}\,[B]_1\,[R]_1^{n-1}\,\{F\}_1 \qquad \text{Eq. (4-10)}$$

Since, as seen from equation (4-10), "Conformal Shrinking" eliminates the need to calculate the $[B]$ and $[R]$ matrices for each iteration, a problem to which this simplification could be applied was chosen to illustrate the "Iterative Shrinking" approach. In the following chapters the problem of a finite crack in an infinite plate is analyzed with this approach.

CHAPTER V

THE PROBLEM OF A FINITE CRACK IN AN INFINITE PLATE

In chapter four it was shown that "Conformal Shrinking" results in a great simplification of the basic equation for "Iterative Shrinking". This approach, however, is limited to geometric structures which, in the limit, approach a point. A typical problem to which "Conformal Shrinking" can be applied is the problem of a crack in a loaded plate. The fundamental case, a line crack in an infinite plate, has a theoretical solution and is, therefore, chosen as an illustrative example primarily to verify the accuracy obtained by the "Iterative Shrinking" approach. In the analysis which follows, the theoretical solution to this problem is presented followed by a "Conformal Shrinking" approach.

Timoshenko and Goodier [1] have solved the problem of uniaxial tension in an infinite plate with an elliptical hole. This problem, which in the limit case is the problem of a finite line crack in an infinite plate, is shown in figure (5-1). The constant tensile load S at infinity are oriented at an arbitrary angle β to the major axis of the ellipse. The foci of the ellipse are at c and -c. In elliptical coordinates the boundary of the ellipse corresponds to

$$\xi = \xi_0 .$$

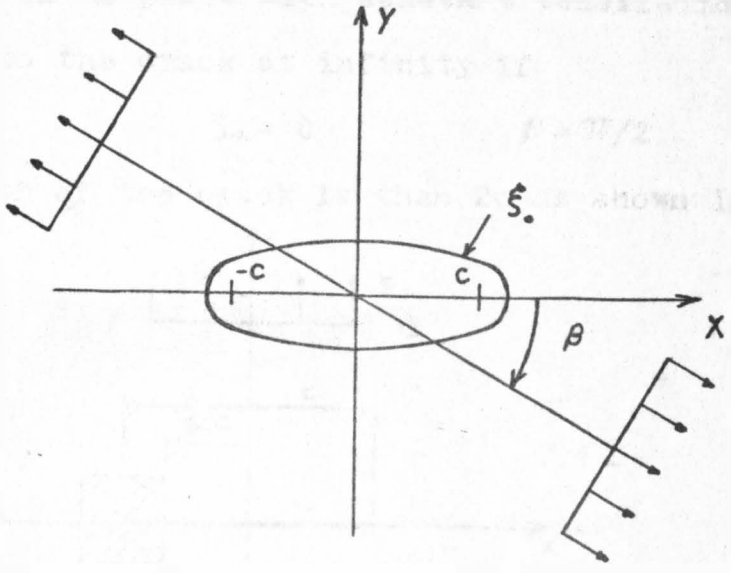

Fig. (5-1) Problem of an elliptical hole in a plate.

The solution to the problem, as shown in reference [1], is given by the complex potentials, $\Psi(z)$ and $X(z)$, where

$$4\Psi(z) = S\ c\left[e^{2\xi_o}\cos 2\beta\cosh\zeta + (1-e^{2\xi_o} + 2i\beta)\sinh\zeta\right]$$

$$4X(z) = -S\ c^2\left[(\cosh 2\xi_o - \cos 2\beta) \quad -\tfrac{1}{2}\ e^{2\xi_o}\cosh 2(\zeta - \xi_o - i\beta)\right]$$

Eqs. (5-1)

and

$$z = x + iy \qquad \text{Eq. (5-2)}$$

$$z = c\cosh\zeta\ . \qquad \text{Eq. (5-3)}$$

The stresses, σ_x, σ_y, and τ_{xy}, are obtained from the complex potentials by the following relations.

$$\sigma_x + \sigma_y = 4\mathrm{Re}\,\Psi'(z) \qquad \text{Eq. (5-4)}$$

$$\sigma_y - \sigma_x + 2i\ \tau_{xy} = 2\left[\bar{z}\,\Psi''(z) + X''(z)\right] \qquad \text{Eq. (5-5)}$$

$$\bar{z} = x - iy \qquad \text{Eq. (5-6)}$$

This problem reduces to that of a finite line crack

in an infinite plate with constant tensile load S perpendicular to the crack at infinity if

$$\xi_o = 0 \qquad \beta = \pi/2 \qquad \text{Eqs. (5-7)}$$

The length of the crack is then 2c as shown in figure (5-2).

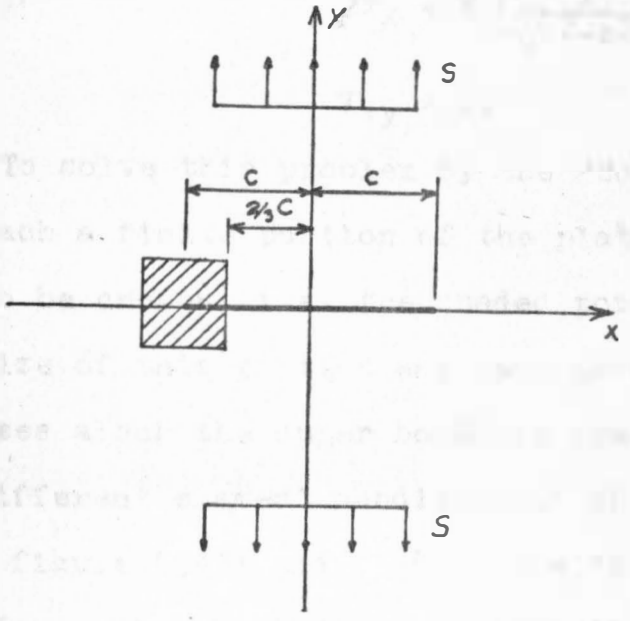

Fig. (5-2) Problem of a crack in an infinite plate.

By differentiating equations (5-1) with ξ_o and β given by equations (5-7) and substituting the derivatives into equations (5-4) and (5-5), it is found that

$$\sigma_x + \sigma_y = S\left[\frac{2z}{\sqrt{z^2-c^2}} - 1\right]$$

$$\sigma_y - \sigma_x + 2i\tau_{xy} = \frac{-Sc^2\bar{z}}{(z^2-c^2)^{3/2}} + \frac{Sc^2 z}{(z^2-c^2)^{3/2}} + S. \qquad \text{Eqs. (5-8)}$$

Since we will be only interested in stresses along the x axis

$$\bar{z} = z = x.$$

Substituting the above values for z and $\bar{z}$ into equations

(5-8) and solving for the stresses, it is found that along the x-axis

$$\sigma_y = \frac{Sx}{\sqrt{x^2-c^2}}$$

$$\sigma_x = S\left[\frac{x}{\sqrt{x^2-c^2}} - 1\right] \qquad \text{Eqs. (5-9)}$$

$$\tau_{xy} = 0.$$

To solve this problem by the "Conformal Shrinking" approach a finite portion of the plate near the crack tip has to be chosen, i.e. the shaded portion of figure (5-2). The size of this portion was made large enough so that the stresses along the upper boundary are nearly constant. Two different element subdivisions of this segment were used, figure (5-3) and (5-4). The "Shrinking Ratio" α and the "Inner Ring Ratio" β were left as parameters to be varied for an optimal solution.

$$\alpha = a/b \qquad \beta = d/a \qquad b = 4$$

The loading along the upper edge is as shown in figure (5-3) and (5-4). The loading is such that it corresponds to a uniform stress of 4 psi. The two edge loads are only half the magnitude of the other loads because it is assumed that half the load at these points is carried by the part of the plate from which this segment was taken. Zero vertical displacements were assumed along the horizontal line of symmetry at nodes 25, 9, 18, 30 for figure (5-3) and at nodes 25, 9, 18, 38, 39, for figure (5-4). In addition,

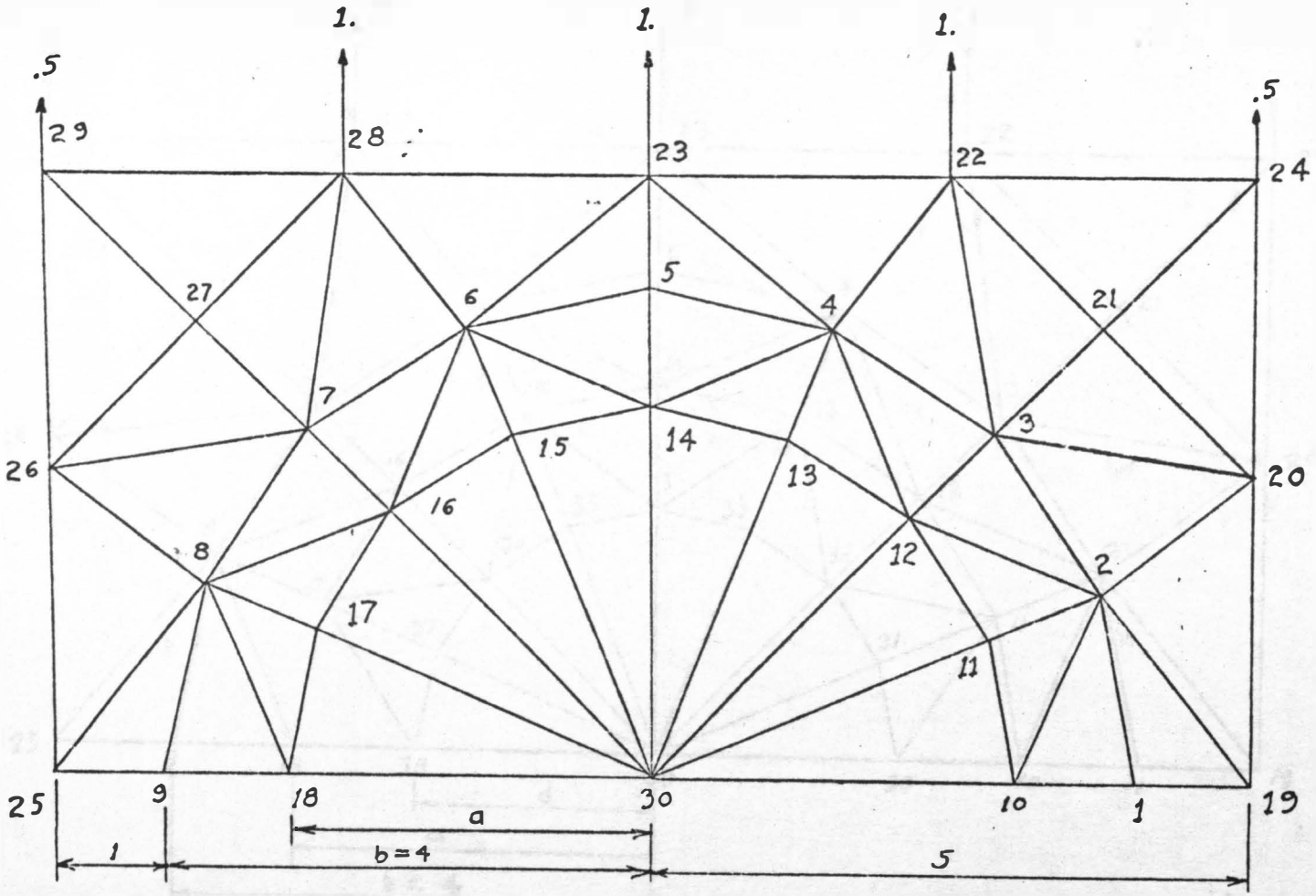

Fig. (5-3) Single ring structure.

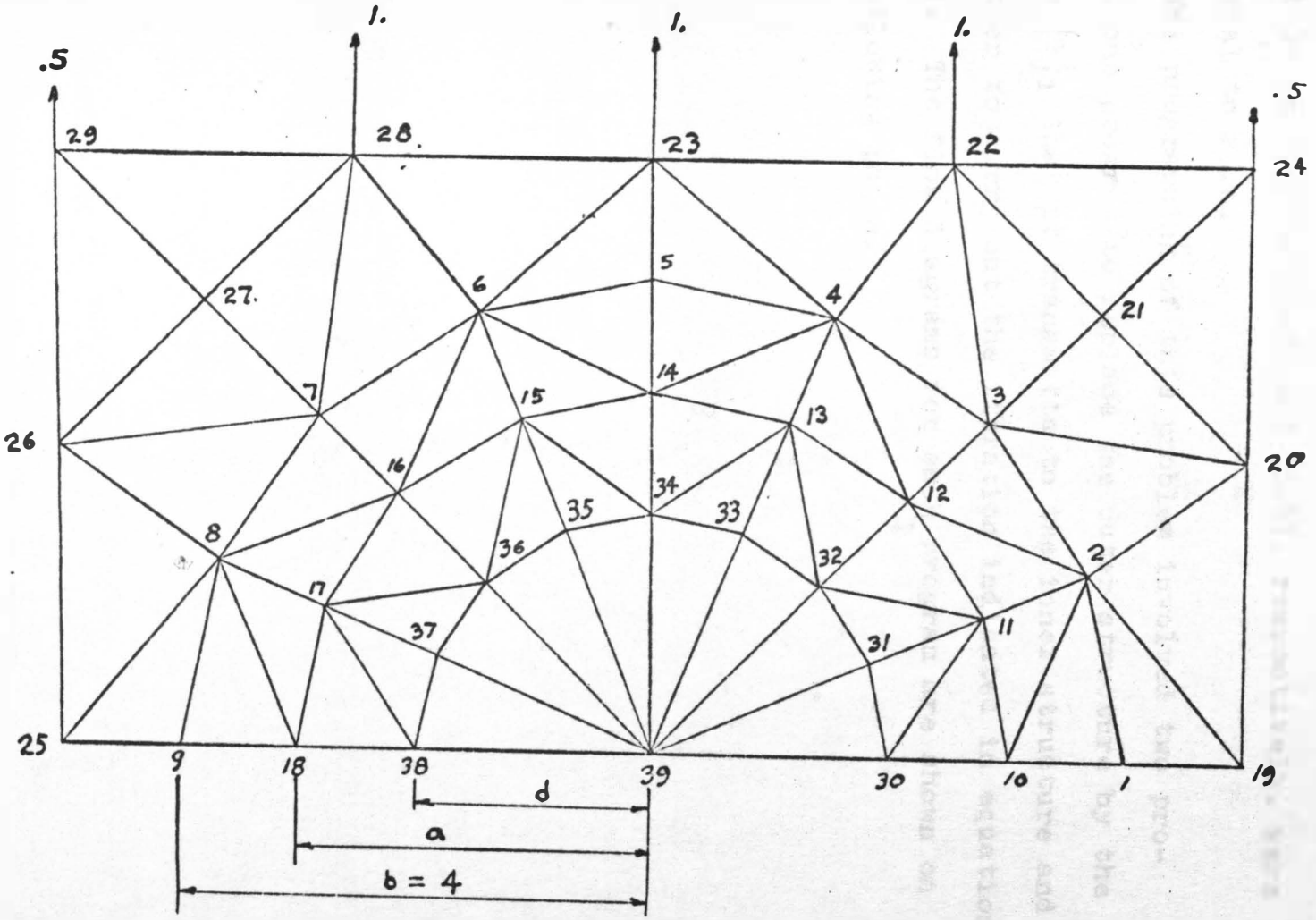

Fig. (5-4) Double ring structure.

one horizontal displacement at the crack tip, or at nodes 30 and 39 in figures (5-3) and (5-4), respectively, were set equal to zero.

The programming of this problem involved two programs, one program to replace the outer structure by the forces $\{F\}_1$ that it transmitts to the inner structure and the other to carry out the iteration indicated in equation (4-25). The flow diagrams for each program are shown on the following pages.

Program to calculate ring loading $\{F\}_1$.

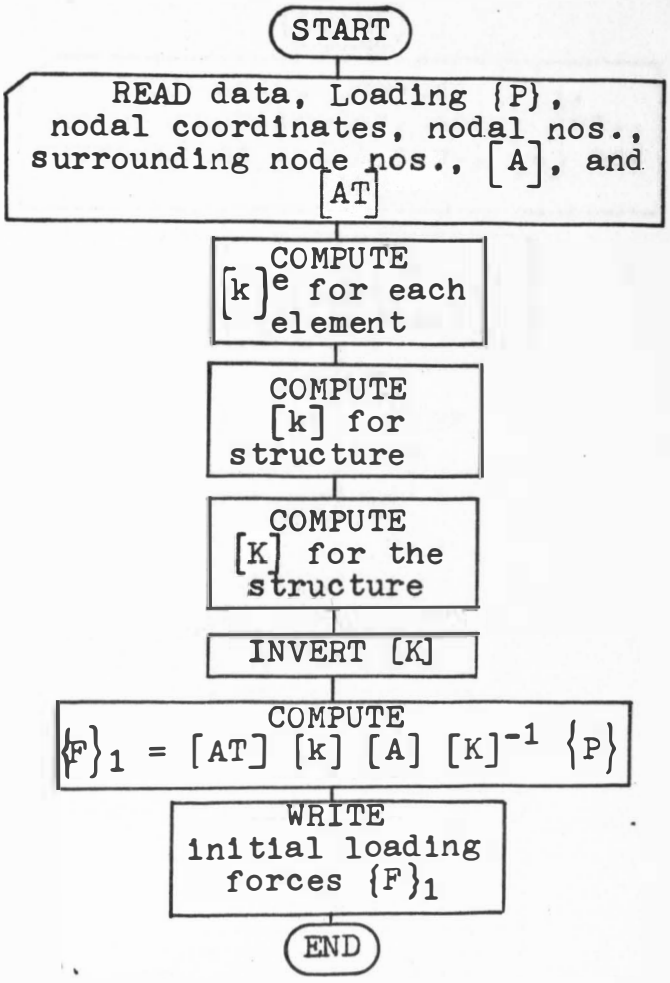

Program to perform iteration.

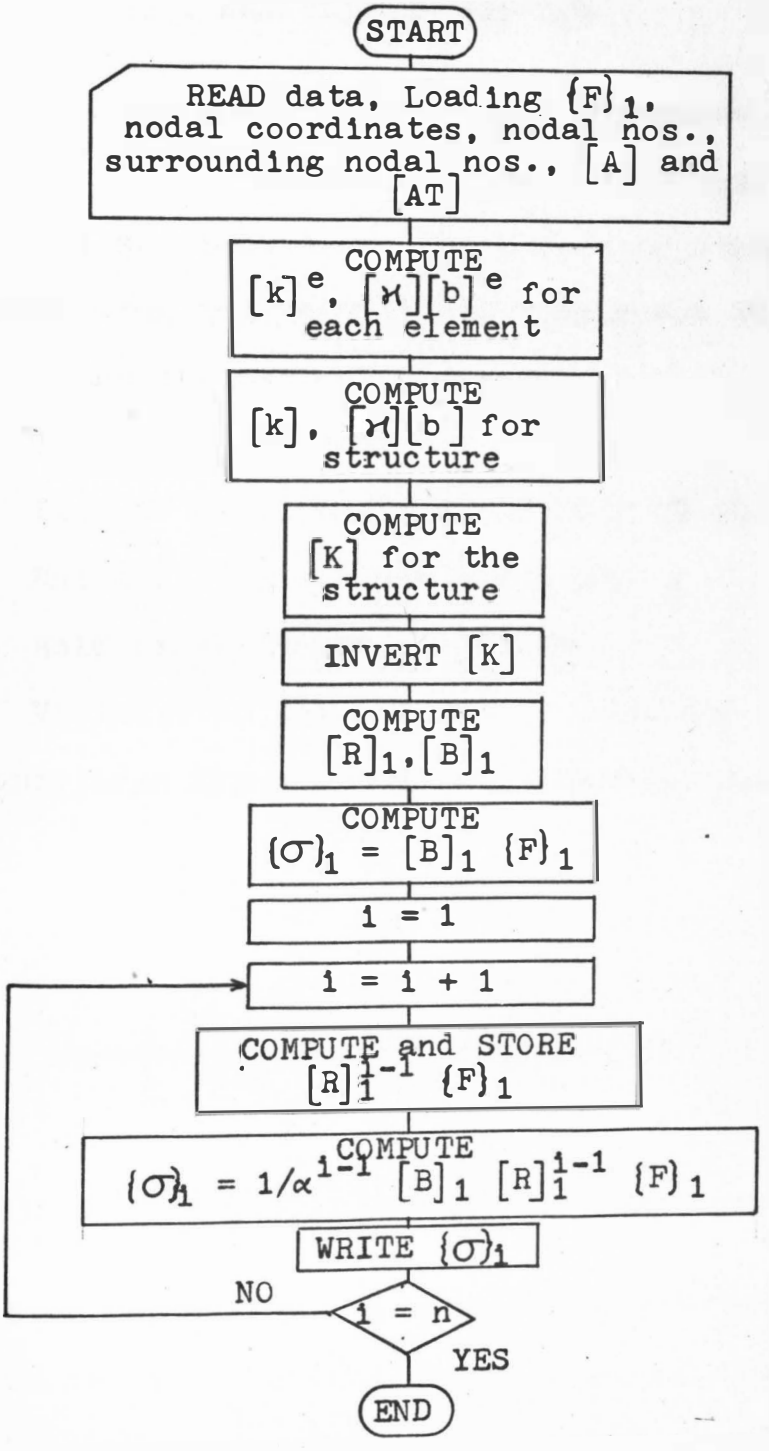

CHAPTER VI

ANALYSIS OF RESULTS

Although the example problem as described in the previous chapter holds for all the cases with similar geometry, regardless of absolute size, the following quantities were used in computing the results for comparison with the ones obtained by the theoretical solution:

(1) Thickness of plate = 0.1 in.

(2) Part of plate analyzed is 10 x 10 in.

(3) Uniaxial stress-load S = 4 psi.

(4) Half crack length c = 15 in.

(5) Vicinity of tip analyzed 0.001 in.

These proportions are shown on the diagram below.

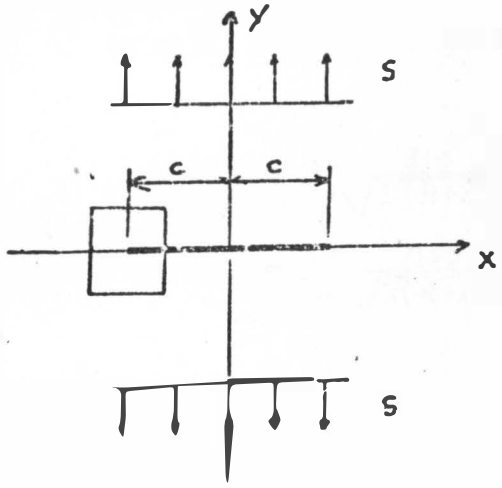

As it is impractical to compare the complete stress fields obtained by "Iterative Shrinking" and the theoretical solution, the comparison was performed by using parameters characterizing the stress fields. The choice of parameters is described in the following paragraphs; it

was kept in mind that the stress distribution near the crack tip is of primary interest.

We have seen in chapter V that the theoretical solution for stresses along the x axis for the problem of a finite line crack in an infinite plate is given by

$$\sigma_y = S \frac{x}{\sqrt{x^2-c^2}}$$

$$\sigma_x = S \left[\frac{x}{\sqrt{x^2-c^2}} - 1\right] \quad \text{Eqs. (5-9) rep.}$$

$$\tau_{xy} = 0.$$

For this analysis it is convenient to introduce R, the distance from the crack tip, where

$$R = x - c$$

$$x = R + c \quad \text{Eq. (6-1)}$$

Substitution of equation (6-1) into equations (5-9) results in

$$\sigma_y = S\left[\frac{R+c}{\sqrt{R(R+2c)}}\right]$$

$$\sigma_x = S\left[\frac{R+c}{\sqrt{R(R+2c)}} - 1\right] \quad \text{Eqs. (6-2)}$$

$$\tau_{xy} = 0.$$

By taking the logarithm of the first of equations (6-2), we see that

$$\text{Log}\,\sigma_y = \text{Log}\,S + \text{Log}\,(R+c) - \tfrac{1}{2}\,\text{Log}\,R - \tfrac{1}{2}\,\text{Log}\,(R+2c) \quad (6\text{-}3)$$

As we approach the crack tip, R in relation to c becomes negligible and, therefore, very near the crack tip

$$\text{Log}\,\sigma_y = k - \tfrac{1}{2}\,\text{Log}\,R \quad \text{Eq. (6-4)}$$

where k is approximately a constant:

$$k = \text{Log } S - \tfrac{1}{2} \text{ Log } 2 + \tfrac{1}{2} \text{ Log } c$$

Also very near the crack tip, the ratio of σ_y to σ_x approaches one as shown below.

$$\frac{\sigma_y}{\sigma_x} = \frac{R+c}{R+c-\sqrt{R^2+2cR}}$$

$$\lim_{R \to 0} \sigma_y / \sigma_x = c/c = 1. \qquad \text{Eqs. (6-5)}$$

As can be seen from equation (6-4), the plot of Log σ_y versus Log R should approach a straight line with a slope of -.5 as we approach the crack tip. One criterion used to compare the accuracy of the "Iterative Shrinking" solution is chosen to be this limit "Slope" of Log σ_y versus Log R. The second criterion is based on equations (6-5). It was chosen as the ratio of σ_y to σ_x as we approach the tip; according to the theoretical solution it should tend to one.

In figure (6-1) is shown a representative plot of Log σ_y versus Log R for both the theoretical and an "Iterative Shrinking" solution. From diagrams similar to the one in figure (6-1) the "Slopes" near the crack tip were obtained for the various "Iterative Shrinking" solutions.

As mentioned in chapter V, for the "Iterative Shrinking" approach, two different element subdivisions near the crack tip were chosen; one with only a single band of elements and one with a double band (see figures (5-3) and (5-4)).

The first division considered was the single band

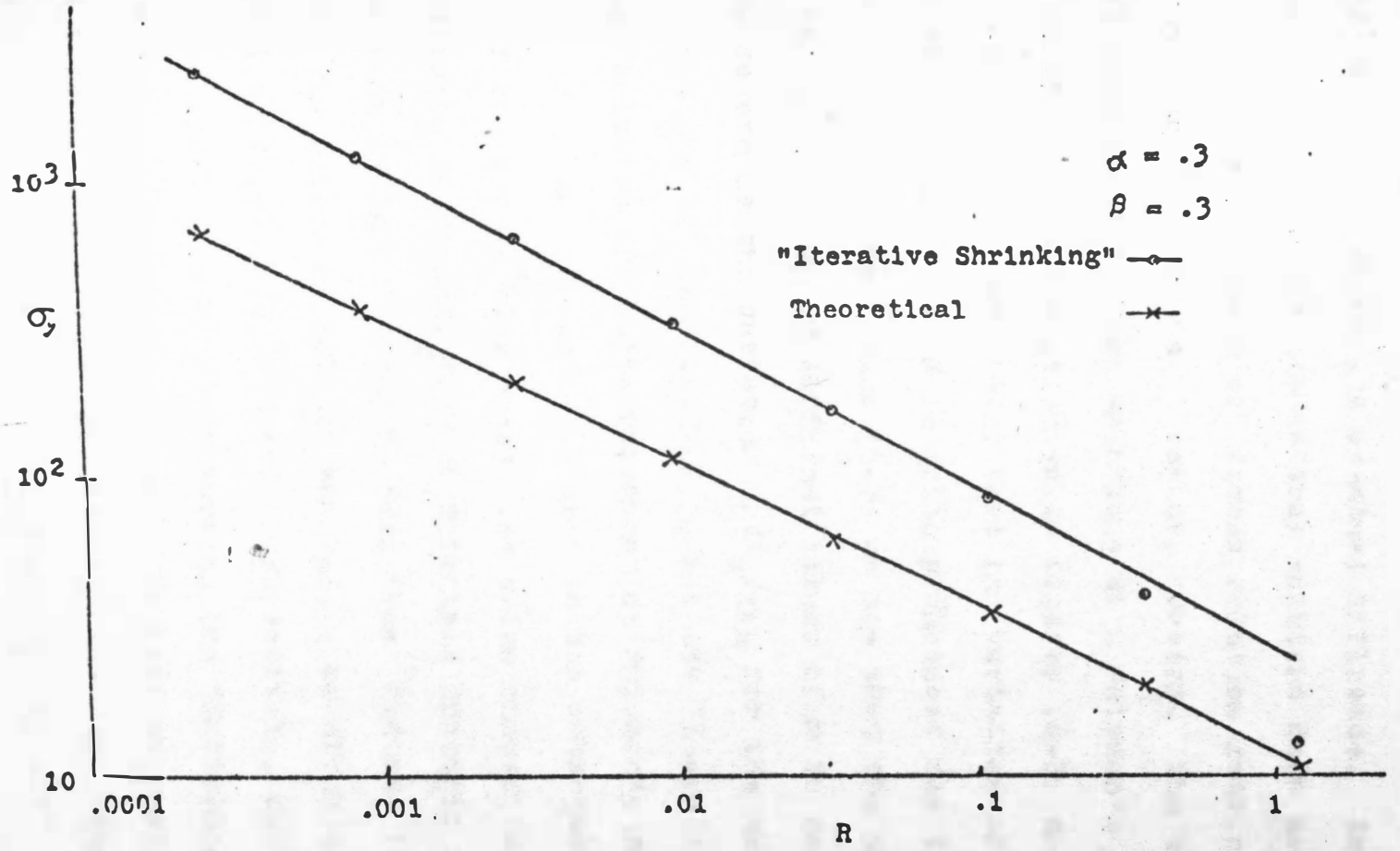

Fig. (6-1) Log Log plot of theoretical and "Iterative Shrinking" solutions.

structure. A series of computing runs were made first with Poisson's ratio ν to check its eventual influence. As seen from equations (6-2), the theoretical solution does not depend on ν. The stiffness and stress relation matrices, $[k]$ and $[\varkappa]$, do contain ν as a factor, however. The variation of the "Iterative Shrinking" solutions with Poisson's ratio for the single ring cases is shown in figures (6-2) and (6-3). It can be seen from figure (6-2) that the variation of σ_y/σ_x with the "Shrinking Ratio" α is quite pronounced for different values of ν. From figure (6-3) we see that the variation of "slope" with α for different values of ν is not nearly as severe as the variation of σ_y/σ_x for the same cases. Since the "Slopes" and σ_y/σ_x for the "Iterative Shrinking" solution are quite dependent on Poisson's ratio ν, a value of .3 was chosen to be used in the subsequent analysis of the double ring cases. The value chosen for Poisson's ratio is roughly that of materials commonly used in engineering design. As can be seen from figures (6-2) and (6-3), the values of "Slope" and σ_y/σ_x as given by the theoretical solution, i.e. -.5 and 1 respectively, differ from all the results obtained by varying the "Shrinking Ratio" α for the single ring cases. The best approximation for this type of geometry is for $\alpha = .75$ ($\nu = .3$). This case would result in a "Slope" = -.83 and $\sigma_y/\sigma_x = 1$.

The next step in the search for a better approximation

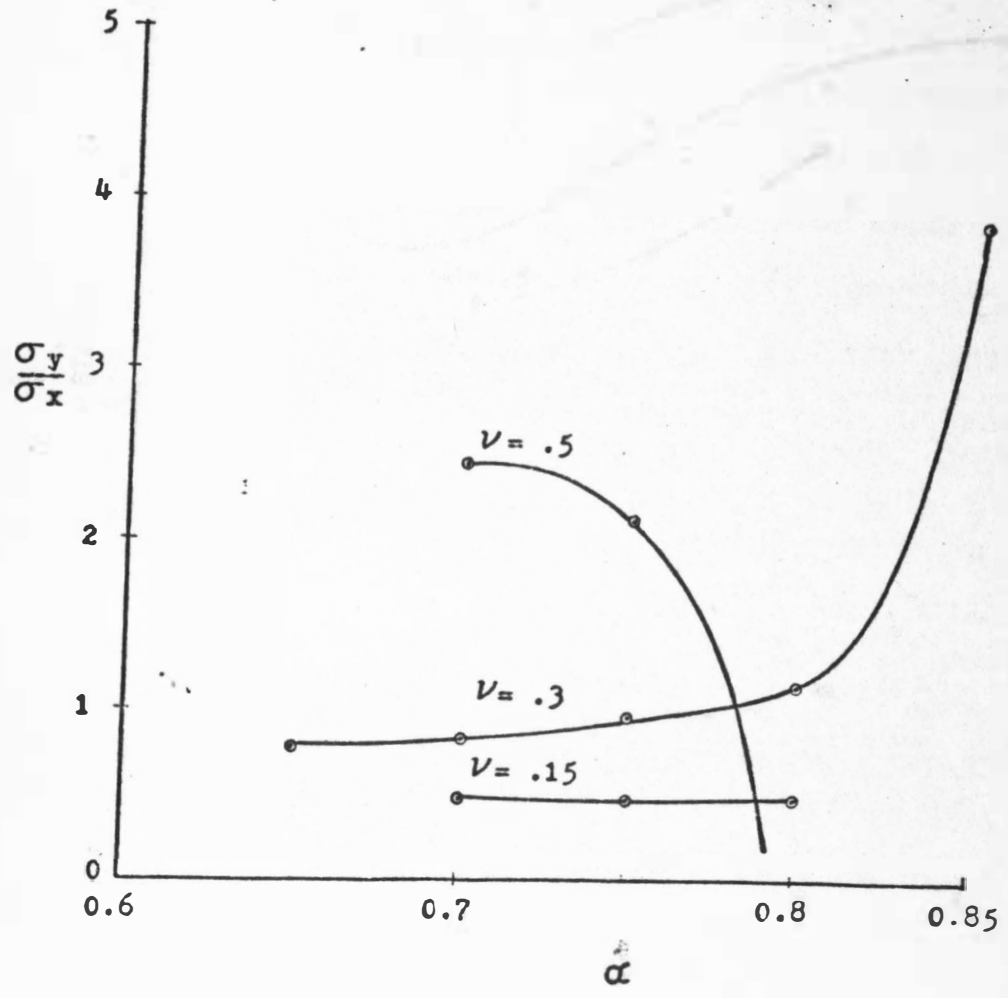

Fig. (6-2) Variations of σ_y/σ_x with Poisson's ratio; (single ring division)

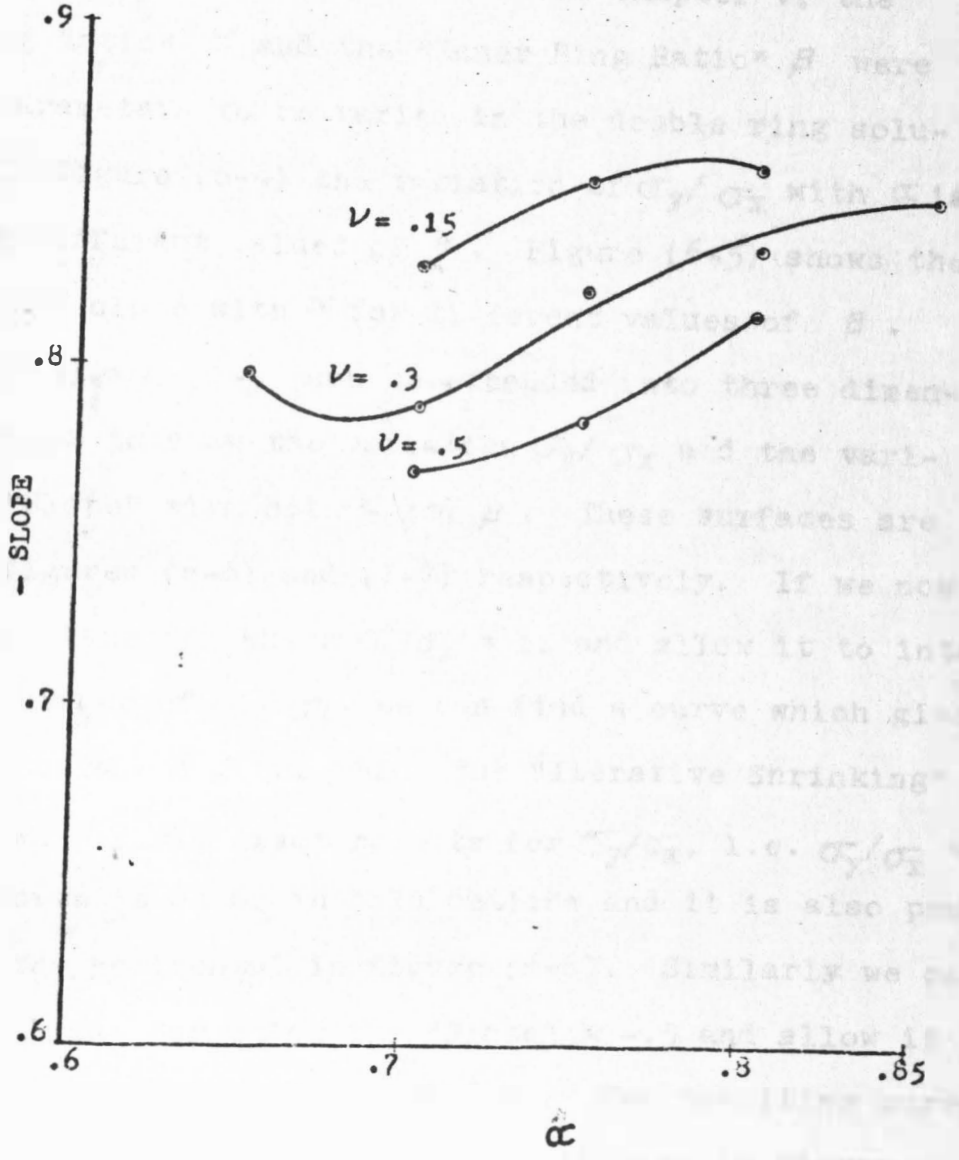

Fig. (6-3) Variations of "Slope" with Poisson's ratio, (single ring division)

to the theoretical solution was to use a finer inner structure. The structure chosen was a double ring structure shown in figure(5-4). As mentioned in chapter V, the "Shrinking Ratio" α and the "Inner Ring Ratio" β were left as parameters to be varied in the double ring solutions. In figure (6-4) the variation of σ_y/σ_x with α is shown for different values of β. Figure (6-5) shows the variation in slope with α for different values of β. Figures (6-4) and (6-5) can be expanded into three dimensional graphs to show the variation σ_y/σ_x and the variation of "Slope" with both α and β. These surfaces are shown in figures (6-6) and (6-7) respectively. If we now choose the plane for which $\sigma_y/\sigma_x = 1$, and allow it to intersect the surface of σ_y/σ_x, we can find a curve which gives the values of α and β for which the "Iterative Shrinking" solutions will yield exact results for σ_y/σ_x, i.e. $\sigma_y/\sigma_x = 1$. This curve is shown in bold outline and it is also projected on the horizontal in figure (6-6). Similarly we can choose the plane for which the "Slope" = -.5 and allow it to intersect the surface of figure (6-7). The resulting curve, shown in a bold outline and on the horizontal in figure (6-7), gives the values of α and β for which the "Iterative Shrinking" solutions will yield exact "Slopes", i.e. Slope = -.5. If these two curves are now superimposed as shown in figure (6-8), it can be checked if there are any values of

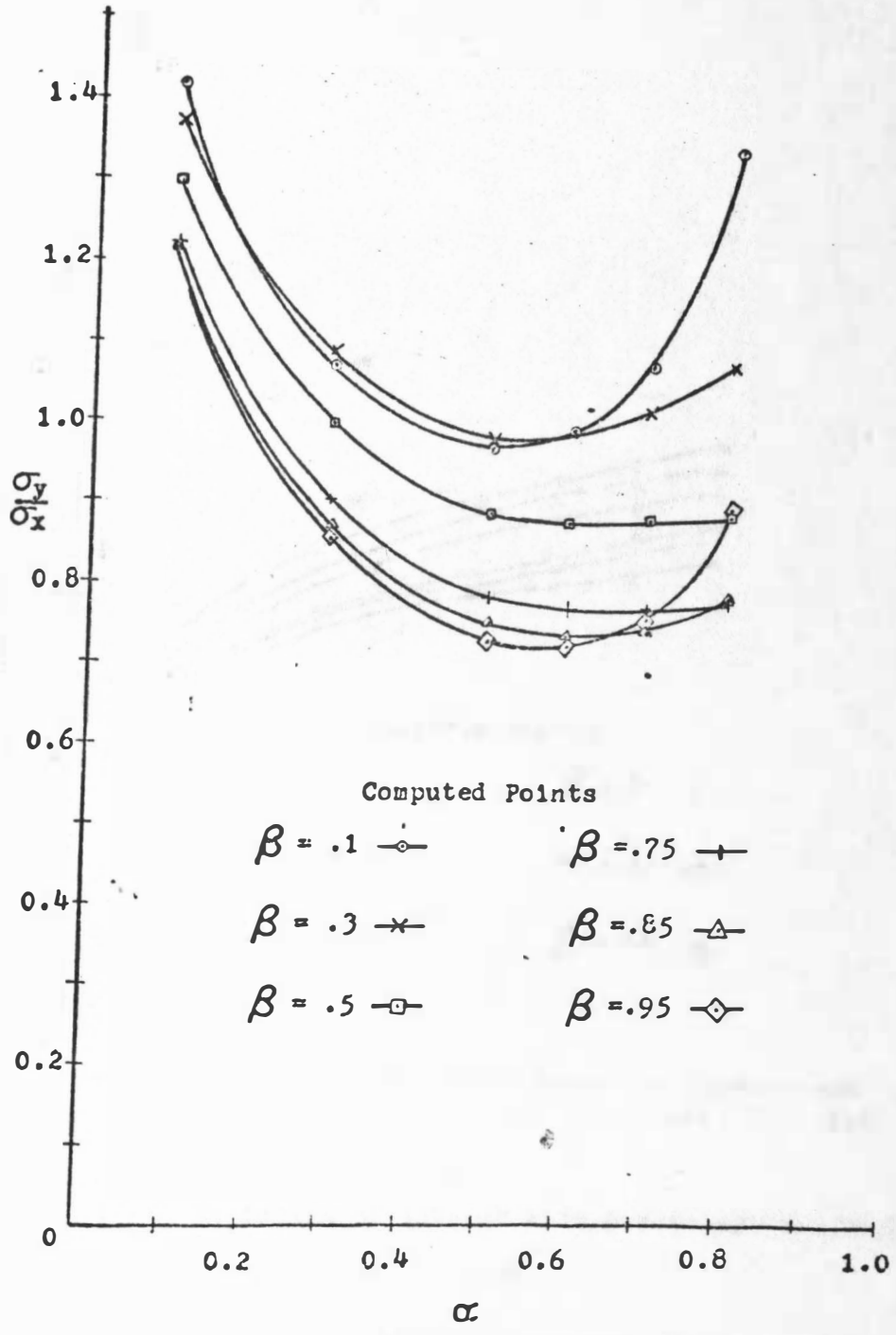

Fig. (6-4) Variation of σ_y/σ_x with parameters α and β; (double ring division)

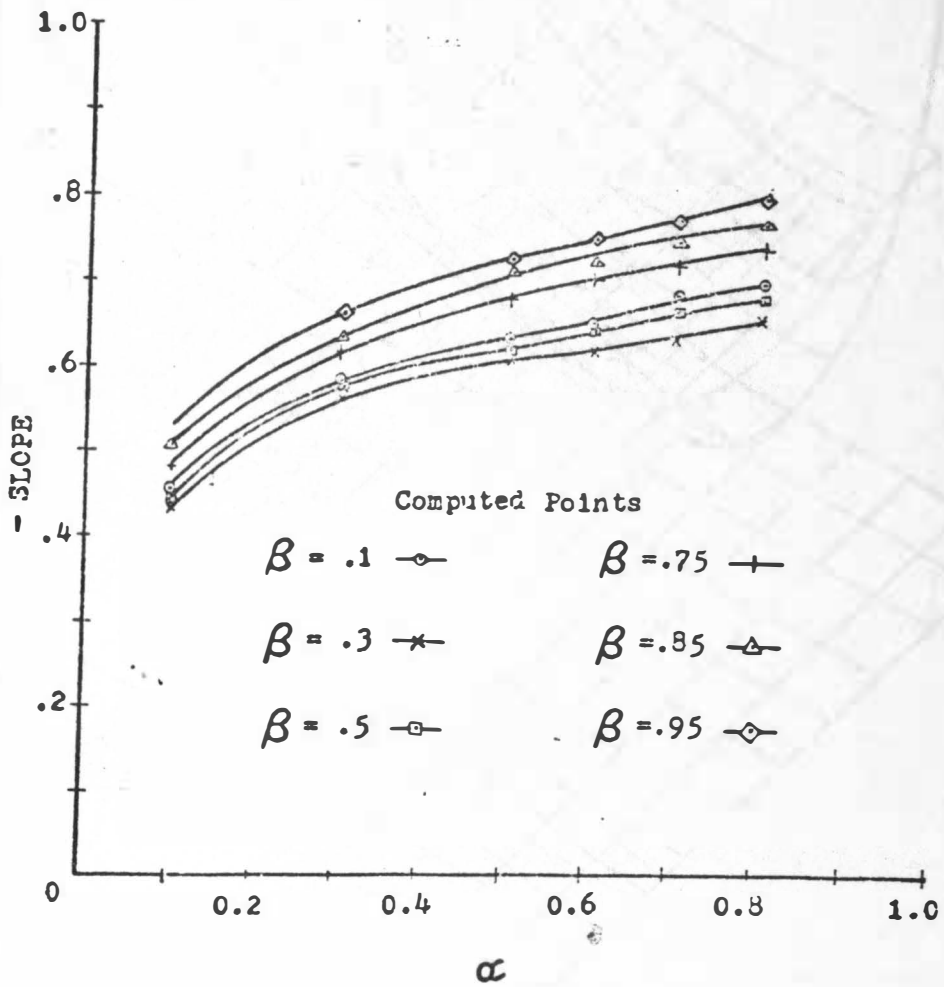

Fig. (6-5) Variation of "Slope" with parameters α and β; (double ring division)

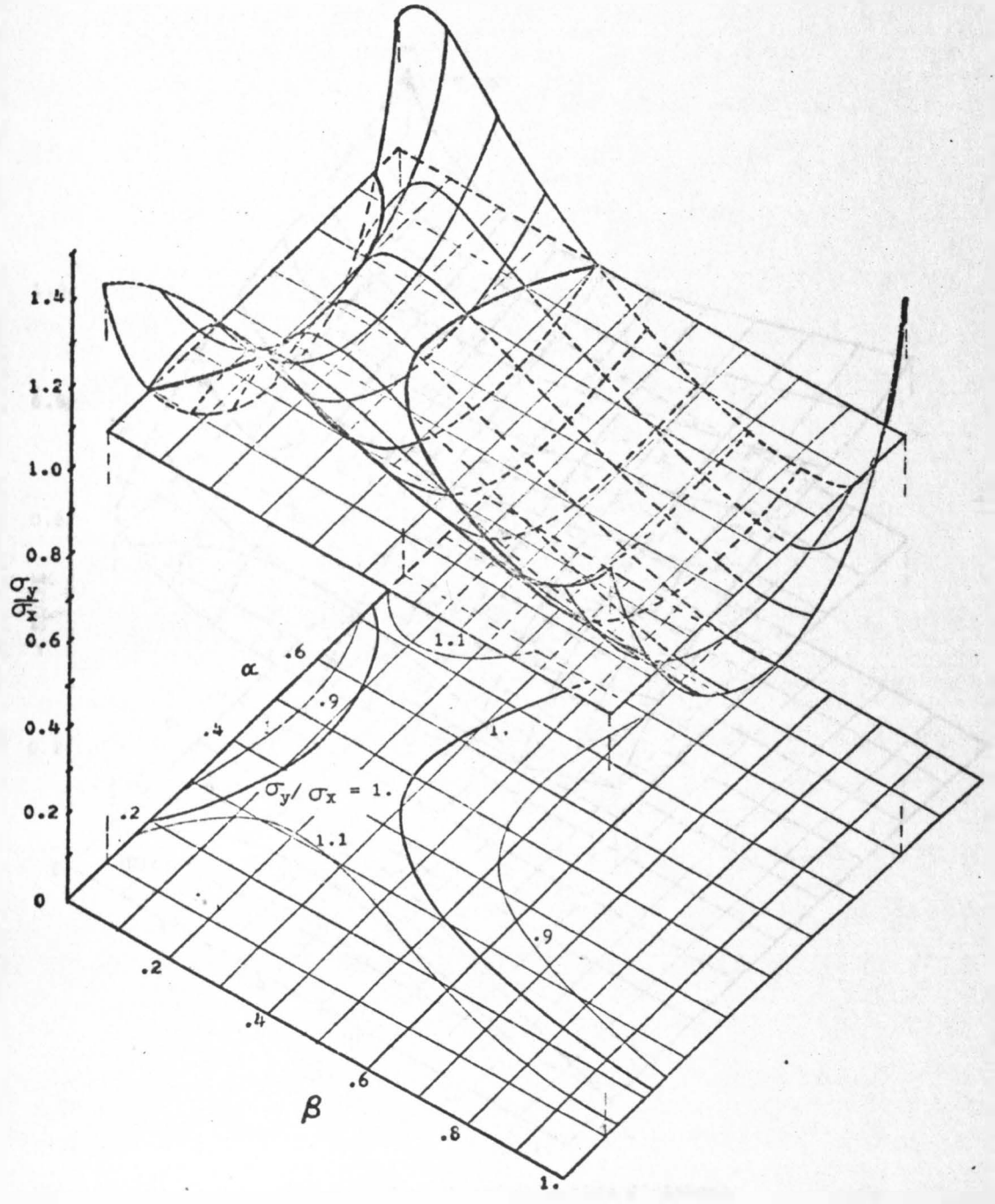

Fig. (6-6) Surface $\sigma_y/\sigma_x = f(\alpha,\beta)$; (double ring division)

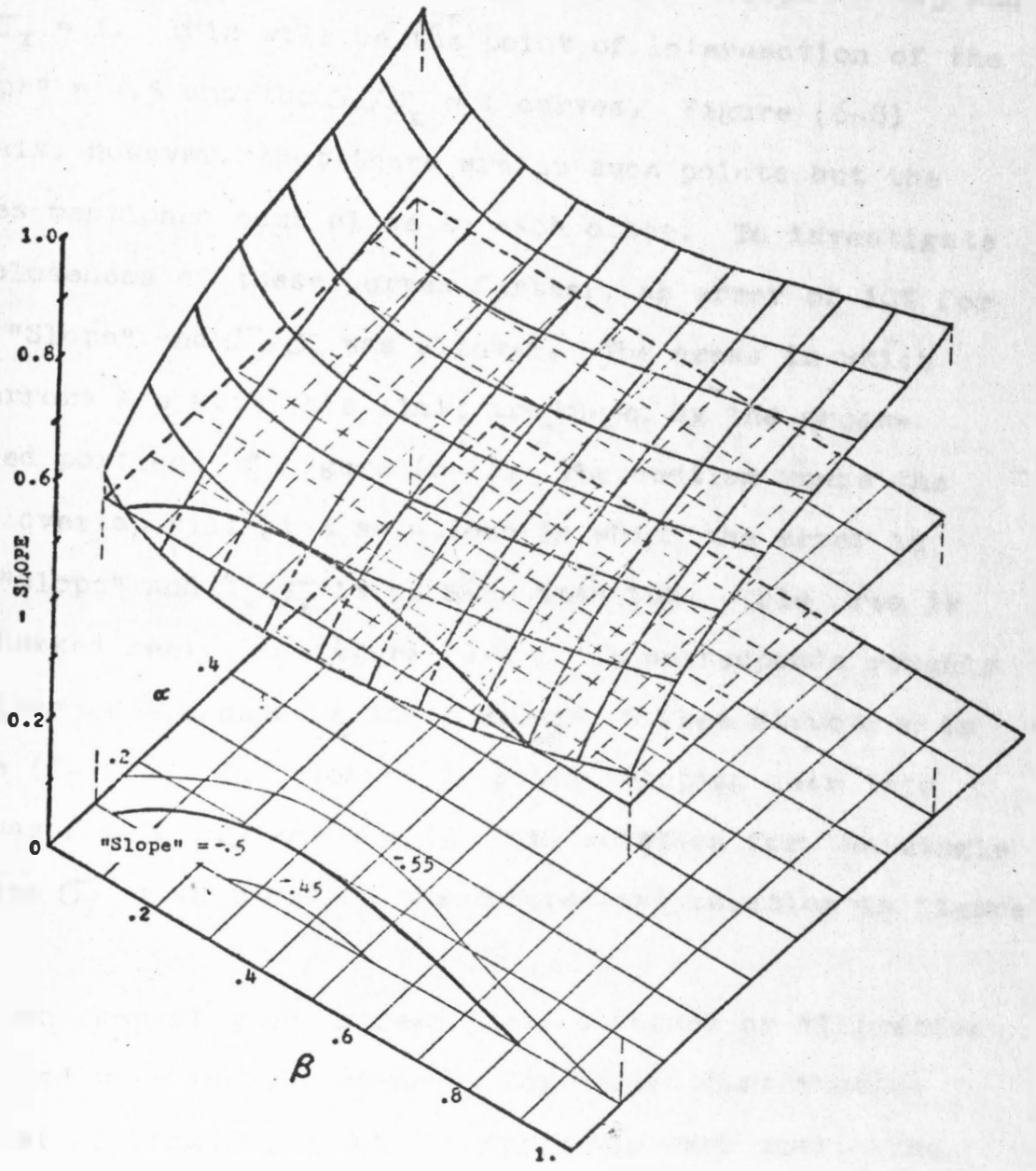

Fig. (6-7) Surface "Slope" = $f(\alpha,\beta)$; (double ring division)

α and β for which the "Iterative Shrinking" solutions will yield both exact "Slopes" and σ_y/σ_x, i.e. "Slope" = -.5 and $\sigma_y/\sigma_x = 1$. This will be the point of intersection of the "Slope" = -.5 and the $\sigma_y/\sigma_x = 1$ curves. Figure (6-8) reveals, however, that there are no such points but the curves mentioned come close to each other. To investigate the closeness of these curves further, an error of 10% for both "Slope" and σ_y/σ_x was allowed. The areas in which the errors are with this limit are shown by the cross-hatched portions of figure (6-8). The section where the areas overlap will give solutions in which the error in both "Slope" and σ_y/σ_x is no more than 10%. This area is the checked region in figure (6-8). It corresponds roughly to values of α around .2 and β around .6 (see structure in figure (6-10)). The closest computed solution near this area was for $\alpha = .3$ and $\beta = .3$. This solution for the single stresses σ_y is compared to the theoretical solution in figure (6-9).

When comparing the stress field obtained by "Iterative Shrinking" with the theoretical, the stress distribution and order of singularity at the crack tip were used. The stress levels on the isolated plate and on the theoretical plate were not related to the same parameter state. This is the reason for the relative vertical shift of the curves that appear in figure (6-9), as each curve has its own factor,

$k = \text{Log } S - \frac{1}{2} \text{ Log } 2 + \frac{1}{2} \text{ Log } c$. The curves from the logarithmic diagram in figure (6-1) are replotted in figure (6-9) where the same difference shows up. This was thought irrelevant for the problem considered as the equilibrium condition itself insures the correct stress level in both cases.

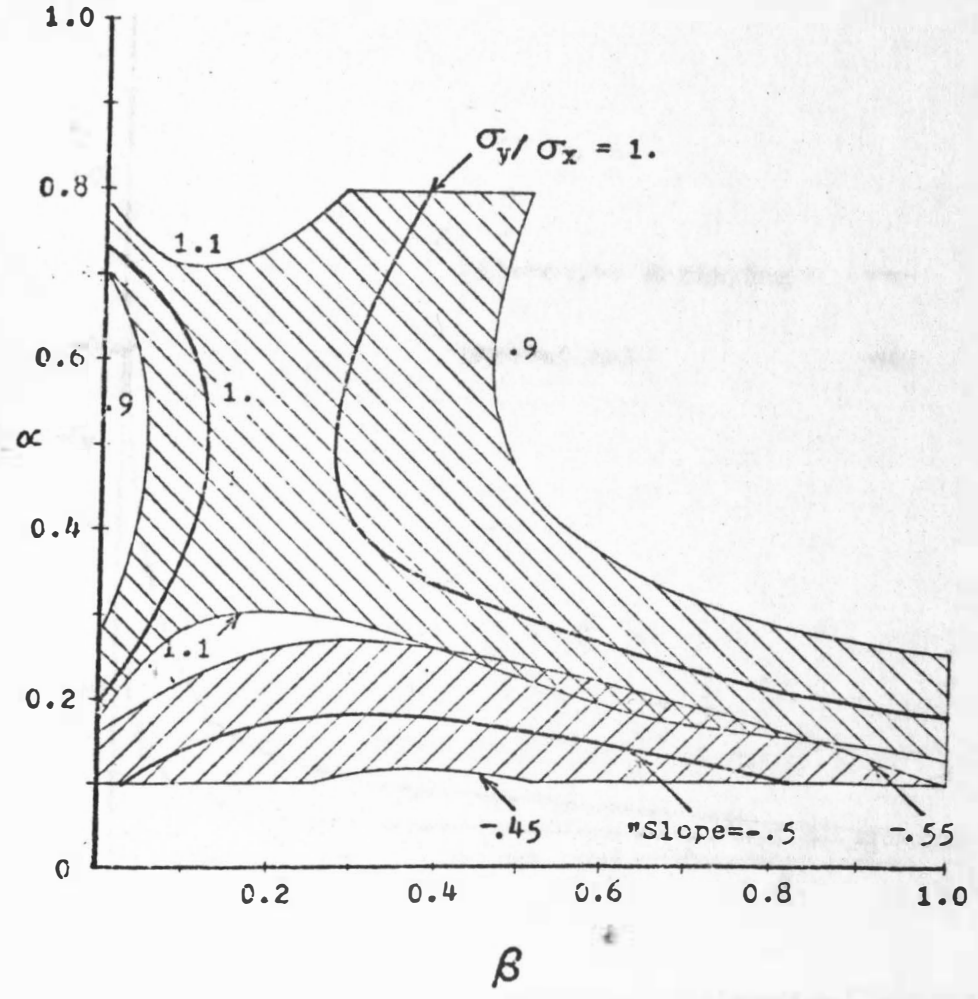

Fig. (6-8) Accuracy areas in α, β plane, (double ring division)

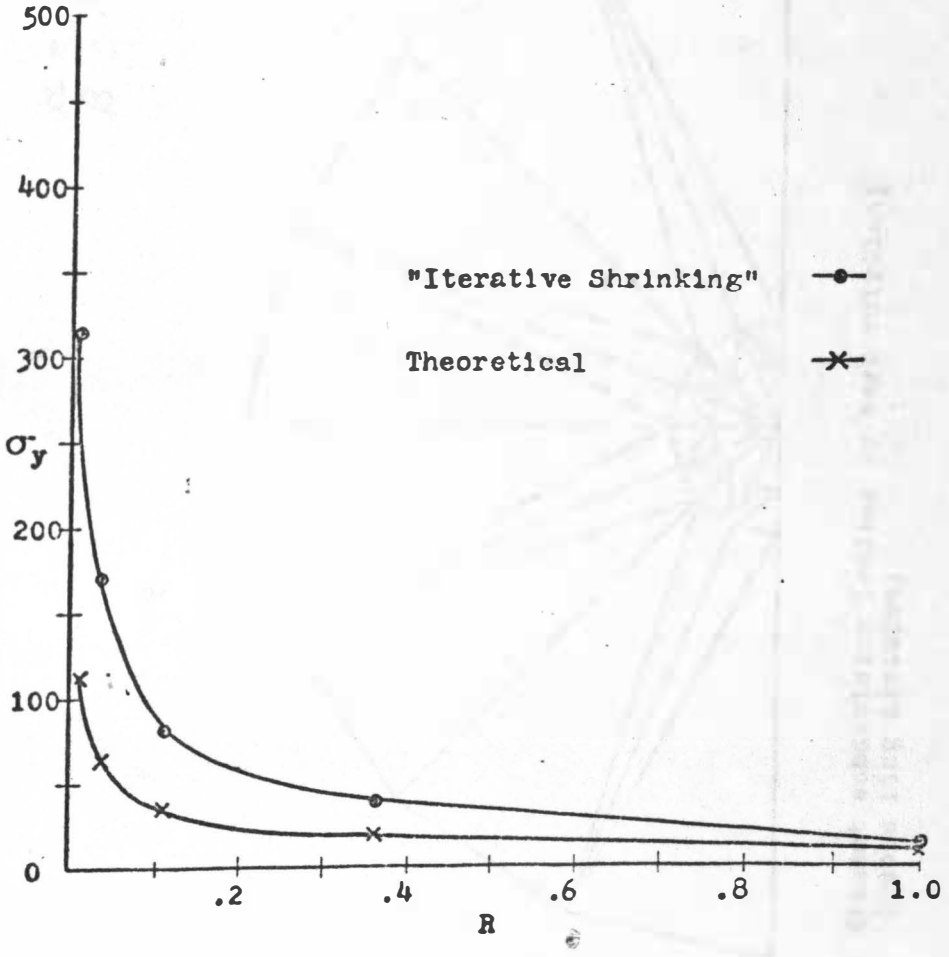

Fig. (6-9) "Iterative Shrinking" and Theoretical solutions for stresses σ_y, (double ring division)

$\alpha = .2$
$\beta = .6$

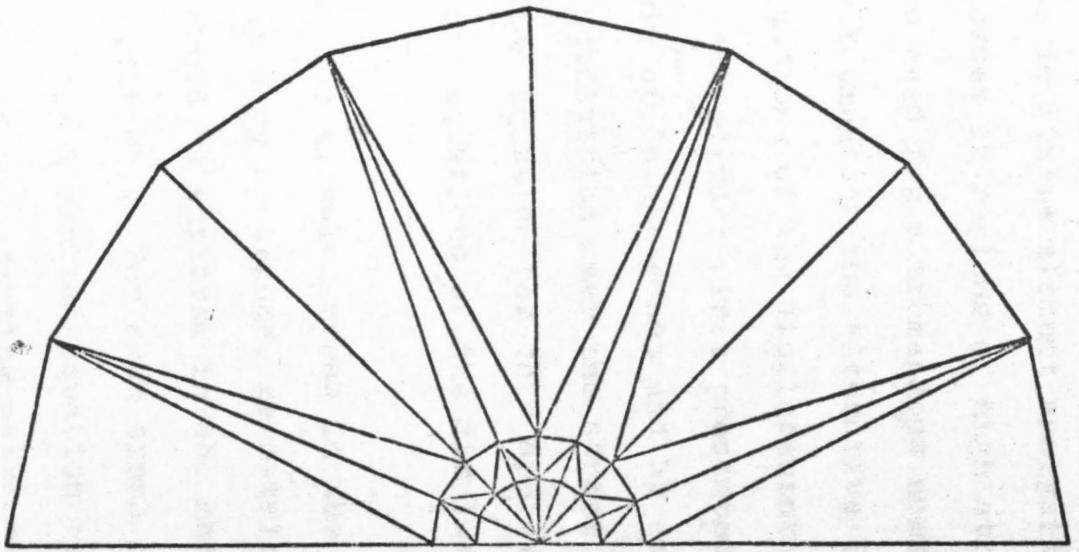

Fig. (6-10) Element subdivision leading to best solution;
(double ring division)

CHAPTER VII

SUMMARY AND RECOMMENDATIONS

The purpose of this thesis was to attempt to develop an iteration technique in finite element analysis that would predict the stresses in regions of high stress concentration without the need for a tremendous number of elements. In the development of the "Iterative Shrinking" approach the basic equations of the displacement formulation of the Finite Element Method were first presented. By employing the principle of Saint-Venant and by choosing a band type of element subdivision near the stress concentration zone, the iteration equation for this approach was developed from the basic equations of the displacement formulation.

It was noted that for singular areas in the stress field, such as sharp corners or cracks, geometrically similar band structures could be employed in the matrix iterations ("Conformal Shrinking"). For such types of structures it was found that the iteration equation reduced to simply the remultiplying of the starting matrices.

The problem of a finite crack in an infinite plate, to which "Conformal Shrinking" could be applied, was chosen to illustrate the "Iterative Shrinking" technique. The "Iterative Shrinking" solutions were compared to the theoretical elastic solutions. Although the solutions obtained vary

with the geometry parameters chosen, the variations are generally around the exact solution. This shows that a useful result can be obtained if the geometry parameters are properly chosen. In the cases considered, the best result would be obtained by using a double band with an outer ring or "Shrinking Ratio" $\alpha = 0.2$ and an "Inner Ring Ratio" $\beta = 0.6$ (such a band structure is shown in figure (6-10)). This result differs from the initial feeling that the ring should represent a "narrow" band of elements. It is actually narrow relative to the singularity of the remaining region.

The solutions presented were obtained by treating the example structure with a relatively coarse element subdivision. This was imposed by the restrictions on the computer time available. It is anticipated that the "Iterative Shrinking" approach would give still better results if a finer mesh were used, as is usually the case in practical applications.

It was concluded in this thesis that (1) the "Iterative Shrinking" approach results in a great savings in computer time and (2) that this method, at least for the problem considered, can be made to closely approximate the type of stress distribution obtained from the theoretical solution.

The conclusions drawn here are based on numerical experimentation as is usual in analyzing a finite element approach. Much more experimentation is, however, needed

before some general conclusion and instructions for the application of "Iterative Shrinking" approach can be made.

REFERENCES

1. Timoshento, S. and Goodier, J. N., Theory of Elasticity, McGraw-Hill Book Company, Inc., 1951, pp. 201-203.

2. Chou, Pei Chi and Pegano, Nicholas J., Elasticity, D. Van Nostrand Company, Inc., 1967, pp. 34-49.

3. Zienkiewicz, O. C. The Finite Element Method in Engineering Science, McGraw-Hill, 1971, pp. 16-31.

4. Przemieniecki, J. S., Theory of Matrix Structural Analysis, McGraw-Hill Book Company, 1968, pp. 61-137.

5. Khol, Ronald, Computer Stress Analysis, Machine Design, November 15, 1969, pp. 85-94.